Applications of in-situ soil moisture observations to better characterize field-level water dynamics

by

Pedro Rafael Rossini Martínez

B.S., Universidad de la República, Uruguay, 2011

A THESIS

submitted in partial fulfillment of the requirements for the degree

MASTER OF SCIENCE

Department of Agronomy
College of Agriculture

KANSAS STATE UNIVERSITY
Manhattan, Kansas

2021

Approved by:

Major Professor
Andres Patrignani

Copyright

Abstract

Water is a relevant input in crop production and represents the second major consumer of freshwater withdraws in United States. In the state of Kansas, a total of 9 million hectares are used for crop production annually, with 1 million hectares being managed in irrigation conditions. In a current scenario facing challenges associated with water shortages and concerns about water use in agriculture, accurate monitoring of rootzone soil moisture has become relevant towards a more efficient use of water in agricultural systems. In this thesis we present and discuss two research questions aimed at improving water use based on soil moisture monitoring in rainfed and irrigated agricultural fields. The first research question that we addressed is: How can we define the number and optimal deployment location of soil moisture sensors in agricultural fields under rainfed and irrigated conditions based on soil moisture-based management zones? This study involved the intensive collection of in situ surface soil moisture observations and soil physical properties across multiple fields. Delineation of soil moisture-based management zones was compared to common proxy variables used to characterize management zones such as soil texture and elevation. A new method to characterize soil moisture-based management zone is proposed in order to objectively define the optimal number and tentative location of soil moisture sensors in crop fields. The second research question that we addressed is: Is it possible to estimate rootzone soil water storage solely based on surface soil moisture observations? In this study we tested a widely used semi-empirical exponential filter model to estimate rootzone soil moisture in agricultural fields using observations from a single soil moisture sensor located near the soil surface. Different rootzone depths were tested and the accuracy of the model was calculated in order to evaluate the feasibility of this model to guide irrigation management. As a general result we propose an objective methodology to guide the deployment of a limited number of soil moisture sensors across crop production fields as well as a method to delineate in-field soil moisture management zones based in soil moisture observations. In addition, we provided useful insights to estimate rootzone soil moisture from near-surface soil moisture observations in agricultural fields.

Table of Contents

List of Figures

List of Tables

Acknowledgements

I would like to acknowledge my wife Paula, who supported and helped me during this new challenge allowing me to grow personally and professionally. I would also like to thank my family for their unconditional love and support. Lastly, I want to thank Dr. Patrignani for coaching me with tireless patience and dedication, pushing me to develop as a thinker and better professional.

Dedication

To my son Felipe who cheers my days and Juana who cheers my near future.

Chapter 1 - General Introduction

Agricultural production is a major user of global water resources and a more efficient use of water resources is critical to ensure food security. Irrigated agriculture is the principal water user at a global scale, accounting for about 70% of the total water withdrawals (FAO, 2021). In the United States, about 25.4 million hectares of agricultural fields and pastures are irrigated, making crop production the second largest consumer of freshwater accounting for 42% of the total freshwater withdraws in 2015 (Dieter et al., 2018). The Ogallala-High Plains Aquifer spans 45 million hectares across eight states in the Great Plains (McGuire, 2012) and has been the major source of freshwater for irrigated agriculture in state of Kansas, which represent 1 million hectares in 2018 (NASS, 2018). Recent studies reported a substantial declining of the water level in the Ogallala aquifer due to excessive pumping for irrigated agriculture (McGuire, 2012). Water shortages have reinforced the importance of water use in agricultural fields and have promoted recent regulations affecting irrigation water use. In this context, better understanding the soil moisture dynamics of agricultural fields has potential to improve water use in agriculture.

Considering available technologies to improve farm-level water management, soil moisture sensors had been proven to be an effective tool to guide the timing and amount of water irrigation, which can result in water savings of up to 50% (Hassanli et al., 2009), while maintaining crop yield and profitability (Evans et al., 2013; Kukal et al., 2020). However, a challenge that remains insufficiently addressed in irrigation scheduling resides in identifying the optimal number and position of a limited number of soil moisture monitoring locations in agricultural fields. In this study we present a new methodology based on clustering classification analysis, temporal stability analysis, and computational geometry to characterize the soil moisture spatial variability of agricultural fields and identify time-invariant soil moisture management zones. In addition, number and optimal soil moisture sensor deployment location is calculated for each field.

Monitoring rootzone soil moisture in agricultural fields can provide valuable information to guide in-season management decisions in rainfed fields and to improve the timing and amount of water applications in irrigated systems. Considering the small sensing volume of traditional point-level sensors, multiple sensors are often required to accurately assess the entire rootzone soil moisture conditions, which becomes laborious, impractical, and can result too costly for local producers. The exponential filter (Wagner et al., 1999) is a semi-empirical model that simplifies the soil water balance using a two-layer approach and has been proven accurate to estimate rootzone soil moisture from surface soil moisture observations in grassland fields (Albergel et al., 2008; Ceballos et al., 2005; Ford et al., 2014). Based on these studies, we hypothesize that a single shallow soil moisture sensor coupled with the exponential filter will result in accurate rootzone soil moisture estimates in agricultural fields. The proposed method is presented in order to determine the accuracy of the rootzone soil water storage prediction compared to a dense array of soil moisture sensors along the soil profile.

References

Albergel, C., ¨ Udiger, C. R., Pellarin, T., Calvet, J.-C., Fritz, N., Froissard, F., Suquia, D., Petitpa, A., Piguet, B., & Martin, E. (2008). Hydrology and Earth System Sciences From near-surface to root-zone soil moisture using an exponential filter: an assessment of the method based on in-situ observations and model simulations. In *Hydrol. Earth Syst. Sci* (Vol. 12). www.hydrol-earth-syst-sci.net/12/1323/2008/

Ceballos, A., Scipal, K., Wagner, W., & Martínez-Fernández, J. (2005). Validation of ERS scatterometer-derived soil moisture data in the central part of the Duero Basin, Spain. *Hydrological Processes, 19*(8), 1549–1566. https://doi.org/10.1002/hyp.5585

Dieter, C. A., Maupin, M. A., Caldwell, R. R., Harris, M. A., Ivahnenko, T. I., Lovelace, J. K., Barber, N. L., & Linsey, K. S. (2018). Estimated use of water in the United States in 2015. *U.S. Geological Survey Circular.* https://doi.org/https://doi.org/10.3133/cir1441. [Supersedes USGS Open-File Report 2017–1131.]

Evans, R. G., LaRue, J., Stone, K. C., & King, B. A. (2013). Adoption of site-specific variable rate sprinkler irrigation systems. In *Irrigation Science* (Vol. 31, Issue 4, pp. 871–887). https://doi.org/10.1007/s00271-012-0365-x

FAO. (2021). Food and Agriculture Organization of the United Natios Statistics Division. FAO. http://www.fao.org/land-water/world-water-day-2021/watergovernance/irrigation-reform/en/

Ford, T. W., Harris, E., & Quiring, S. M. (2014). Estimating root zone soil moisture using near-surface observations from SMOS. *Hydrology and Earth System Sciences*, *18*(1), 139–154. https://doi.org/10.5194/hess-18-139-2014

Hassanli, A. M., Ebrahimizadeh, M. A., & Beecham, S. (2009). The effects of irrigation methods with effluent and irrigation scheduling on water use efficiency and corn yields in an arid region. *Agricultural Water Management*, *96*(1), 93–99. https://doi.org/10.1016/j.agwat.2008.07.004

Kukal, M. S., Irmak, S., & Sharma, K. (2020). Development and application of a performance and operational feasibility guide to facilitate adoption of soil moisture sensors. *Sustainability (Switzerland), 12*(1). https://doi.org/10.3390/su12010321

McGuire, V. (2012). Water-Level and Storage Changes in the High Plains Aquifer, Predevelopment to 2011 and 2009–11. *Publications of the US Geological Survey*. https://digitalcommons.unl.edu/usgspubs/123

NASS, U. (2018). Irrigation and Water Management Results from the 2018 Irrigation and Water Management Survey. USDA NASS 2018 *Irrigation and Water Management Survey (2017 Census of Agriculture)*. www.nass.usda.gov/AgCensus

Wagner, W., Lemoine, G., & Rott, H. (1999). A method for estimating soil moisture from ERS Scatterometer and soil data. Remote Sensing of Environment, 70(2), 191–207. https://doi.org/10.1016/S0034-4257(99)00036-X

Chapter 2 – A Quantitative Method to Guide the Number and Location of Soil Moisture Sensors

This chapter will be submitted to Vadose Zone Journal

Abstract

Site-specific irrigation management is becoming a growing priority to improve the use of limited fresh water resources. Soil moisture sensors are useful tools that can lead to a more efficient use of water by improving the timing and amount of irrigation events. However, methods for guiding end users determining the number and location of soil moisture sensors per field still remains poorly explored in the scientific literature. The objective of this study was to develop a quantitative method to determine the minimum number and tentative deployment location of soil moisture sensors (SMS) within agricultural fields based on soil moisture-based management zones (MZ). Multiple intensive surveys of surface (0-12 cm) soil moisture were conducted during the fallow periods of 2017, 2018, 2019 on three agricultural fields in central Kansas using a calibrated hand-held soil water reflectometer. The fuzzy-c means (FCM) clustering method was used to delineated the MZ based on the set of georeferenced soil moisture surveys and the Silhouette clustering evaluation method was used to identify the optimal number of MZ per field. Then, a sensor location index that considered the distance to the MZ boundaries and the FCM membership grade was proposed to identify the tentative optimal deployment location of SMS. Undisturbed surface soil samples were also collected to determine the soil water retention curve and plant available water capacity of each MZ. The proposed method was effective to characterize portions of the field with distinct soil moisture regimes in all three fields and also revealed complex soil moisture spatial patterns that were not captured with elevation or soil texture alone. Dividing the fields using soil moisture-based MZ reduced the intra-zone soil

moisture spatial variability by about 50% compared to that of the entire field. Wet MZ presented on average 14% higher effective water content at saturation, 38% higher soil water content at field capacity, and 207% higher soil moisture content at the permanent wilting point compared to dry MZs. Our method indicates that a total of two soil moisture sensors seems to be sufficient to capture most of the soil moisture spatial variability. Future studies aiming at optimizing the number and deployment location of soil moisture sensors should explore soil moisture interactions with deeper soil layers across root-zone to provide a better understanding of the sub-surface spatial variability.

Introduction

In-situ soil moisture sensors (SMS) provide scientists and stakeholders with field-specific and timely information that can be used to guide in-season management decisions in rainfed (e.g. amount of fertilizer and seeding rate) and irrigated (e.g. irrigation scheduling) agricultural systems. In the United States, the adoption of soil moisture sensing technologies remains low, with only ~11% of the U.S. farms using soil moisture sensing devices (Kukal et al., 2020). But, with the increasing need for sustainable use of water resources and the advent of more affordable and reliable soil moisture sensing technologies, the adoption of SMS by producers, irrigation water managers, and researchers is expected to increase in the near future. New SMS offer innovative sensor designs, practical installation methods, and convenient on-board wireless data telemetry (e.g. radio frequency, cellular networks, and local long-range wide-area networks) (Ding and Chandra, 2018) that adapt to a wide range of consumer needs and are enabling the deployment of local field-level soil moisture networks for precision irrigation scheduling (Hedley et al., 2012). However, a challenge that remains insufficiently addressed in the scientific literature resides in identifying the optimal number and position of a limited number of soil moisture monitoring locations in agricultural fields, a problem that largely depends on discerning field areas with clearly defined and temporally stable soil moisture spatial patterns.

A major consideration when deploying an array of soil moisture sensors is the limited scalability of the resulting monitoring system. Installing soil moisture sensors in agricultural fields often requires manual soil trenching or soil augering, deployment of additional hardware for data collection and telemetry that can conflict with frequent farming operations, and in some cases additional soil sampling to develop a local sensor calibration. As a result, the installation of soil moisture sensors is often approached as a semi-permanent setting (i.e. few to several growing seasons), where delineation of zones with more homogeneous soil moisture conditions relative to that of the entire field seems to be the preferred and most cost-effective alternative. Traditionally, the delineation of field management zones (MZ) has been aimed at guiding the application of fertilizers based on spatial patterns of yield in combination with surface soil chemical properties (i.e. soil pH, phosphorus, organic matter) (Schepers et al., 2004), apparent soil electrical conductivity in combination with soil particle size and elevation (Fraisse et al., 2001; Peralta et al., 2015; Reyes et al., 2019), yield maps collected over multiple growing seasons and different phases of the crop rotation (Basso et al., 2007), and using remote canopy reflectance indices (e.g. NDVI) from satellite platforms (Boydell and Mcbratney, 2002). In recent years, advancements in the variable rate irrigation technology coupled with the increasing need to optimize irrigation efficiency to conserve surface and groundwater resources has increased the focus on delineation of MZ with emphasis on soil moisture (Haghverdi et al., 2015; C. Hedley et al., 2009; Sadler et al., 2005). However, existing research on this area heavily relies on proxy variables for soil moisture rather than actual soil moisture observations. For instance, delineation of site-specific MZ for irrigation scheduling typically includes multiple combinations of apparent soil electrical conductivity, elevation, topographic indices (e.g. wetness index), and soil texture (Boluwade et al., 2015; Hedley and Yule, 2009; Moral et al., 2010; Reyes et al., 2019); remote sensing vegetation indices (e.g. NDVI) (Reyes et al., 2019; Haghverdi et al., 2015); and characterization of soil water holding capacity (Hedley and Yule, 2009; Oldoni and Bassoi, 2016; Zhao et al., 2018). Despite the close link between these variables and soil moisture, we were unable to find any study in the scientific literature that considered the delineation of MZ strictly based on spatially-intensive in situ soil moisture observations.

While less common in agricultural fields, frequent and spatially intensive soil moisture surveys have proven useful in catchment-level studies to reveal the primary factors controlling the temporal and spatial soil moisture patterns. For instance, daily measurements of surface (0-5 cm) soil moisture at 1-meter intervals along a hillslope transect in a watershed near Austin, TX revealed that on wet conditions soil moisture patterns were mainly driven by soil porosity and hydraulic conductivity, but during dry conditions the major controlling factors were elevation, slope aspect, and clay content (Famiglietti et al., 1998). Another study involving the collection of intensive surface (0-30 cm depth) soil moisture observations in the Tarrawarra catchment in Victoria, Australia, demonstrated that seasonal soil moisture patterns were associated with both random and topographic variation, and to some extent, soil moisture patterns exhibited a limited correlation with soil type and soil hydrologic parameters (Western and Grayson, 2000). These complex transient interactions between soil moisture, extrinsic landscape properties, and highly variable intrinsic soil properties operating even within seemingly homogeneous landscape units demonstrate that neither the use of a single soil or landscape feature, nor the use of a single soil moisture survey may be sufficient to accurately characterize the soil moisture spatial variability of small catchment areas. Similarly to landscapes dominated by grassland vegetation, large commercial agricultural fields can also span diverse landscape positions and soil types. Since information about the soil moisture spatial variability based on in situ observations already reflects the compounded effect of extrinsic and intrinsic variables, delineating MZ using in situ soil moisture observations has the potential to remove much of the uncertainty associated with using proxy variables. Therefore, we hypothesize that the delineation of MZ directly using soil moisture observations will elucidate field spatial patterns that cannot be detected using proxy variables.

A common approach to delineate MZ based on spatial features for agricultural applications is the use of unsupervised clustering. Two of the most common clustering methods for delineating MZ include the K-means (MacQueen, 1967) and Fuzzy C-means (FCM) (Bezdek, 1981) clustering. A distinct advantage of the FCM over K-means is that FCM allows any data point to present partial membership to different clusters (i.e. soft clustering) instead of assigning data points to mutually exclusive clusters (i.e. hard clustering). This unique feature typically makes FCM the preferred method to characterize continuous variables such as soil moisture, soil physical and chemical properties, and crop yield (Burrough, 1989). FCM has been used for generating MZ for variable rate irrigation (Boluwade et al., 2015; Haghverdi et al., 2015; Yari et al., 2017), variable rate nitrogen applications (Peralta et al., 2015), characterization of soil moisture temporal dynamics (Reyes et al., 2019), and to guide the collection of soil samples in representative field areas (Yan et al., 2007). In this study we merged concepts from FCM clustering, temporal stability analysis, and computational geometry to identify time-invariant MZ based on soil moisture observations obtained from multiple intensive field surveys. The goal of this study was to develop a quantitative protocol to determine the i) minimum number of SMS per field and ii) the tentative deployment location of SMS within each agricultural field.

Materials and Methods

Experimental fields

The study was conducted in three agricultural fields located in central Kansas during the fallow periods of 2017 (Field A), 2018 (Field B), and 2019 (Field C) (Table 1). Field A is located near the town of Gypsum, KS and has an area of 28 hectares. The farming operation of Field A is based on a no-tillage crop rotation consisting of annual row crops (corn and soybeans) and alfalfa under rainfed conditions. During this study the crop rotation was in the phase of the annual crops. The predominant soils consist of deep, well-drained, alluvial soils with slopes <1% corresponding to the silt clay loam Detroit series (fine, smectitic, mesic pachic argiustolls) and silt loam Hord series (fine-silty, mixed, superactive, mesic cumulic haplustolls) (Soil Survey Staff, 2020). Field B is located near the city of Hutchinson, KS and has an area of 58 hectares. The cropping system of Field B consists of a minimum tillage operation based on irrigated corn and soybeans under a center pivot. This field is characterized by an rolling terrain dominated by deep loamy alluvium soils corresponding to the Avans series (fine-silty, mixed, superactive, mesic udic argiustolls) with 2 to 4 % slope and aeolian sandy loam soils corresponding to the Saltcreek series (fine-loamy, mixed, superactive, mesic udic argiustolls) with 3 to 5 % slope (Soil Survey Staff, 2020). The rolling terrain has a strong impact on the velocity and direction of runoff water flow in this field, which leads to areas of the field with pronounced rill erosion and localized accumulation of stubble after large rainfall events. Field C is also located in the central portion of Kansas near the town of Moundridge, KS. The field has an area of 22 hectares and the cropping system is based on continuous no-till irrigated corn. This field has an upland area characterized by deep and moderately well drained Crete series (fine, smectitic, mesic pachic udertic argiustolls) with silt loam soils with <1% slopes. The bottom slope is characterized by the Farnum series (fine-loamy, mixed, superactive, mesic pachic argiustolls) with loam soils and slopes ranging from 1 to 3% and with the presence of fine gravel in the top soil horizon (Soil Survey Staff, 2020). The region encompassing the three fields has an approximate average annual rainfall of 800 mm, a mean annual temperature of 13 ºC, and a mean minimum and maximum air temperature of -1 ºC and 27 ºC (Kansas Mesonet, 2021). The region belongs to the Köppen climate class with humid continental hot summers with year round precipitation.

Soil moisture surveys

Soil moisture was measured in the top 12 cm of the soil profile using a hand-held soil water reflectometer (HydroSense II CS659, Campbell Scientific, Logan, UT, USA). The Hydrosense is a light-weight portable sensor that consists of two 12-cm long stainless steel rods attached to an epoxy sensor head. The sensor is connected to a display equipped with an onboard GPS receiver (± 3 m accuracy) that is used for logging the soil moisture readings, the timestamp, and the associated geographic coordinates of each observation. The sensor also stores raw variables such as the apparent dielectric permittivity, which was used to develop a custom sensor calibration equation for accurate determination of volumetric water content. Field measurements of soil moisture were concentrated during the fallow periods to minimize the interference of frequent irrigation events and actively growing vegetation in the determination of soil moisture patterns (e.g. Hupet and Vanclooster, 2002). Fallow periods also facilitated the manual collection of soil moisture observations during the intensive surveys, a task that would have been more labor intensive and time-consuming in the presence of standing crops and frequent irrigation events.

Each intensive soil moisture survey consisted of collecting georeferenced observations in the top 12 cm of the soil profile following a rough grid (Table 1). In total we conducted 16 soil moisture surveys across the three agricultural fields from May 2017 to June 2019, totaling 4659 observations (Table 1). A custom sensor calibration was developed in laboratory conditions using bulk soil from different areas of the fields. The bulk soil was first air-dried, then ground to pass a 2-mm sieve, and then packed into cylindrical containers (2980 cm^3) to create soil columns with known volumetric water content. A linear model was developed relating the apparent dielectric permittivity measured by the sensor with the observed volumetric water content of the containers (Ledieu et al., 1986):

$$\theta = -0.0994 + 0.0968\sqrt{K_a} \quad [1]$$

where θ (m^3 m^{-3}) is the volumetric water content, K_a (unitless) is the real part of the apparent dielectric permittivity, and the two empirical coefficients were determined from the curve fitting exercise using the *lsqcurvefit* function in Matlab 2018b (Mathworks, Natick, MA).

Determination of soil physical properties

In order to characterize the fraction of sand, silt, and clay across the agricultural fields we collected a total of 113, 91, and 106 disturbed soil samples from the top 12 cm across Fields A, B, and C, respectively. The number of samples collected per field was related to the available workforce during the sampling period and the susceptibility to data sparsity of the spatial interpolation method. Based on previous studies, a value of about 100 observations is recommended for spatial interpolation with ordinary kriging (Saito and Goovaerts, 2003). Disturbed soil samples were collected using a shovel and then homogenized in a plastic container before bagging the samples. Soil samples were oven-dried at 105 ºC for 48 hours and ground to pass a 2 mm sieve. Particle size analysis was conducted using the hydrometer method (Gavlak et al., 2003). To characterize the soil water retention properties of each management zone, we collected 18 undisturbed soil samples in the 0-5 cm layer using 250 cm^3 stainless-steel rings. The laboratory procedure for measuring soil water retention curves consisted of first saturating each soil sample in a 5 mM calcium chloride solution. After reaching saturation, each sample was mounted on a sensor head equipped with two precision pressure transducers and two mini-tensiometers (2.5 cm and 5 cm long) (Hyprop 2, Meter Group Inc., Pullman, WA, USA) connected to a desktop computer. The soil matric potential of each mini-tensiometer was recorded using the Hyprop-View software (Meter Group Inc.) while the samples remained exposed to evaporation at laboratory ambient conditions (T=23 ± 2℃, RH=21% ± 5%) (Schindler, 1980; Wind, 1966). Sample mass recorded three times per day during the first three days of the sample drydown and twice a day during the remaining period. Measurements with the Hyprop 2 were terminated after the longer mini-tensiometer (i.e. closest to the sample surface) reached their cavitation point. The next step consisted of dismounting the samples from the Hyprop 2 and then extracting small soil sub-samples along the wetting front of the sample to determine soil water potential using a dewpoint soil water potential meter (WP4C, Meter Group Inc., Pullman, WA, USA). Soil samples were weighed individually and oven dried to obtain the gravimetric water content of each sample. Data were exported and a soil water retention model (van Genuchten, 1980) was fitted using the *lsqcurvefit* function in Matlab 2018b (Mathworks, Natick, MA). To quantify the osmotic potential of the soil solution, six samples per field were measured using the soil water potential meter. The soil solution was obtained from centrifugation of 5 g of ground and oven-dried soil and 5 ml of de-ionized water into a 10 ml centrifuge tube for 30 minutes at 2500 RPM. Similar to previous studies (Bittelli and Flury, 2009), the osmotic potential of all samples was below the detection limit of 0.01 MPa of the instrument, so we assumed that the readings of soil water potential were approximately equal to the soil matric potential.

Determination of the number of management zones

Field-level soil moisture from the intensive surveys was estimated using ordinary kriging. The first step of the spatial interpolation process consisted of detrending the field observations using a quadratic linear regression model based on field coordinates. Then, the residuals for each point in the survey were used to generate an empirical semivariogram and spherical, exponential, and Gaussian semivariogram models were fitted using ordinary least squares. The model with the lowest root mean squared error (RMSE) was selected to represent the spatial dependence in the interpolation step. In this study we assumed an isotropic semivariogram. The exponential model resulted in the best fit in 62% of the cases (10 out of 16), while the spherical model was the best fitting model in the remaining 38% of the cases (6 out of 16) (Table 2). The fitted semivariogram model for each survey was used to interpolate the detrended field soil moisture observations using ordinary kriging method into a 5 m regular grid. The grid spatial resolution was defined so that the 5th percentile of the distances between sampling points of a given survey was represented by at least four pixels (Hengl 2006). Across most field surveys, a value of 5 m provided a reasonable approximation for the size of each grid cell, while providing sufficient spatial detail and maintaining computational performance during the interpolation process. The kriging routine was implemented in Matlab and was used with a local search neighborhood with a maximum of 500 m and a maximum of 15 neighboring observations. Interpolated grids of soil moisture for each survey were normalized relative to the field average, following the same approach commonly used in time stability analysis (Vachaud et al., 1985):

$$\beta_{ij} = \frac{\theta_{ij} - \overline{\theta_j}}{\overline{\theta_j}} \qquad [2]$$

where, β_{ij} is the soil moisture relative difference at location *i* at time *j*, θ_{ij} is the volumetric water content in location *i* at time *j*, and $\overline{\theta_j}$ is the average field volumetric water content at time *j*. To contrast the classification of MZ between in situ soil moisture observations and proxy variables, we also included in the analysis auxiliary variables such as the percent of sand content, percent of clay content, and elevation that were also normalized using Eq. 2 before the clustering analysis.

Because the FCM clustering method requires specifying the number of clusters as input, we combined the FCM clustering method with the Silhouette method (Rousseeuw, 1987) to evaluate the optimal number of MZ per field given a set of normalized variables in raster format. The Silhouette method computes the mean separation Euclidean distance between all grid cells classified within a cluster and evaluates the interclass similarity among grid cells in other clusters, hence the resulting silhouette value serves as an objective metric to define the optimal number of zones per field. Silhouette values range between -1 and 1, where higher values indicate the optimal number of clusters. In our case, silhouette values were computed for a range between 1 and 6 clusters, which spans the typical range of site-specific MZ in agricultural fields. In the special case in which the end goal is not to deploy the least number of SMS, but rather deploying a pre-defined number of SMS (e.g. following budget constraints), this step involving the Silhouette method can be skipped and a pre-defined number of clusters can be enforced in the FCM clustering technique.

The FCM is a widely used clustering technique to partition heterogeneous agricultural fields into more homogenous MZ (Yari et al., 2017; Peralta et al., 2015; Reyes et al., 2019).The FCM is defined as a soft clustering where members (i.e. grid cells in our case) can belong to more than one cluster. Each grid cell in the field is assigned a membership grade in the continuous range from zero to one according to the degree of similarity with other grid cells of the same cluster. A value of one represents perfect membership and a value of zero represents complete lack of membership to a specific cluster. The FCM clustering was implemented using the Matlab function *ffcmw* from the Maltab File Exchange (Cococcioni, 2020). The similarity of the delineated MZ solely based on in situ soil moisture surveys was compared to the delineated MZ based on alternative variables using the Jaccard similarity index. The Jaccard index quantifies the degree of similarity between two finite sets (i.e. two MZ) and is a widely used method to compare the results of image segmentation analysis. The Jaccard index is formally defined as the size of the intersection divided by the size of the union of two finite sets:

$$J(A,B) = \frac{A \cap B}{A \cup B} \qquad [3]$$

where *J(A,B)* is the Jaccard index between sets A and B, $A \cap B$ represents the intersection, and $A \cup B$ represents the union between the two sets. The Jaccard index ranges from 0 to 1, where a similarity of one means perfect matching between the two sets and a similarity of zero represents complete discrepancy between the two sets. The analysis was conducted using the *jaccard* function from the Matlab Image Processing Toolbox v10.3.

Determination of the location of soil moisture sensors

To objectively define the optimal sensor location within each delineated MZ, we defined a sensor location index (SLI) that accounts for both the FCM membership grade and the distance-to-edge of the MZ for each grid cell:

$$SLI_i = agmax \frac{D_i}{D_{\max}} U_i \qquad [4]$$

where SLI_i is the sensor location index at grid cell *i*, D_i is the Euclidean distance from grid cell *i* to the nearest boundary of the delineated management zone, $D_{\max}$ is the maximum Euclidean distance of any grid cell in the delineated zone to the nearest boundary of the zone (i.e. distance of the centermost grid cell of the zone), and U_i is the membership grade at the grid cell *i*. In other words, the SLI finds the center-most grid cell weighted by the membership grade. Both, the distance (D_i/D_{max}) and membership (U_i) components of the SLI are continuous and range between 0 and 1, meaning that the resulting SLI is also bounded in the range [0,1] and is comparable across different MZ. Then, the tentative geographic coordinates for the optimal sensor location in each delineated zone can be found by searching the grid cell with the maximum SLI value (Eq. 4). The proposed method assumes that a single and optimally located SMS can represent the soil moisture conditions of the entire MZ. The assumption rests on the notion that the zoning process substantially reduces the soil moisture spatial variability within each delineated MZ (Barker et al., 2017; Reyes et al., 2019). A distance transform was used to compute the Euclidean distance between each grid cell and the zone boundaries used the Matlab function *bwdist* from the Image Processing Toolbox v10.3 (Maurer et al., 2003). We considered the distance to the edge of the MZ because of two reasons: i) edges of agricultural fields are usually exposed to frequent traffic resulting in higher soil compaction that can affect soil water redistribution and storage, and ii) boundaries between zones constitute transitional zones that may not fully represent either zone (e.g. membership grades around a value of 0.5). Elevation data for each field was obtained from U.S. Geological survey digital elevation models (U.S. Geological Survey, 2017) at 10 m spatial resolution and downscaled to a 5 m grid using a cubic spline interpolation method to match the field grid.

Results and Discussion

Field-level soil moisture spatial variability

Field-average surface soil moisture across all surveys ranged from 0.247 to 0.388 $m^3\ m^{-3}$, with a minimum survey value of 0.123 $m^3\ m^{-3}$ and maximum survey value of 0.483 $m^3\ m^{-3}$. Overall, Field B exhibited drier average soil moisture conditions than Fields A and C, with mean values ranging between 0.247 m^3 m^{-3} to 0.314 m^3 m^{-3} (Table 2). These drier surveys in Field B were likely associated to the predominance of sandy loam and loam soils (Table 3) with low soil water holding capacity. On the other hand, Field C had wetter field-average soil moisture conditions than Fields A and B, with mean survey values ranging from 0.323 m^3 m^{-3} to 0.388 m^3 m^{-3} (Table 2). Wetter conditions in Field C were likely associated to the high field-average clay (26.0%) and silt (50.6%) content. Across all surveys, the CV ranged between 6.8% and 20.3% showing a relatively strong (R^2=0.76, Table 2) inverse linear relationship with field-average soil moisture. The range of observed CV in this study is similar to values observed by Tague et al. (2010) working on a watershed upland forest in Baltimore, USA, and by Brocca et al. (2007) working in several grassland sites (<9,000 m^2) in central Italy. In our study, the highest CV of 20.3% corresponded to the field survey on 5 June 2019 in Field B (Table 2, Figure 1b), with a field-average soil moisture of 0.247 m^3 m^{-3}. Despite this survey being the driest in our dataset, a value of 0.247 m^3 m^{-3} typically represents intermediate soil moisture conditions in these type of fine-textured soils. At intermediate soil moisture conditions, the soil moisture spatial variability is known to be jointly dominated by micro-topography and particle size distribution (e.g. clay content). On the other hand, the lowest CV of 6.8% was observed in the wettest field survey on 8 April 2019 in Field C (Table 2, Figure 1c), where soil moisture spatial variability is known to be dominated by soil physical properties such as soil porosity and hydraulic conductivity (Famiglietti et al., 1998). Our results are consistent with previous studies across multiple geographic regions including central Italy, the southern U.S. Great Plains, New Zealand, and Victoria, Australia, in which the soil moisture spatial variability is greatest at intermediate soil moisture conditions (~0.25-0.30 m^3 m^{-3}) and lower at near saturation soil moisture conditions (Brocca et al., 2007; Famiglietti et al., 2008; Hedley and Yule, 2009b; Western et al., 2003).

Another relevant feature of the statistical analysis of soil moisture surveys is their probability distributions. We found that only 8 out of the 16 surveys passed the Shapiro-Wilk normality test. Non-normal surveys were characterized by high kurtosis, with typical values ranging from 3 up to nearly 7, and by negative skewness with values typically below -0.5. In general, kurtosis values tended to increase whereas skewness values tended to decrease with increasing field-average soil moisture conditions (Table 2). Further inspection of the surveys revealed that in Field C only 1 out of the 7 surveys was normally distributed, with surveys in Field C showing some of the highest kurtosis (from 2.3 to 6.7) and lowest skewness (from 0.09 to -1.5) values across all surveys. Field C was characterized by four clearly defined soil textural classes (Figure 5) and by well-defined upland and lowland areas, the interaction of which resulted in areas of the field with contrasting soil moisture conditions that resulted in heavy-tailed distributions. Our results agree well with those obtained by Famiglietti et al. (1999), who also found increasing kurtosis and decreasing skewness with increasing soil moisture conditions during intensive sampling campaigns in a watershed in central Oklahoma. In a subsequent study monitoring surface soil moisture across six spatial extents ranging from 2.5 m to 50 km in watersheds in central Oklahoma and Iowa, Famiglietti et al. (2008) found a general decrease in skewness from positive to negative values with increasing areal mean soil moisture content.

In our study, the soil moisture spatial dependence was analyzed by fitting semivariogram models to empirical semivariograms using all the points in each survey. Soil moisture surveys exhibited a nugget-to-sill ratio <25%, which can be considered as a strongly spatially dependent process dominated by intrinsic properties such as soil texture and mineralogy (Cambardella et al., 1994). The median level of spatial autocorrelation was concentrated at distances of 180, 150, and 280 m for Fields A, B, and C. The shortest range value of 77 m observed on 8 April 2019 and the largest range value of 792 m observed on 5 April 2019 were both achieved in Field C in surveys only three days apart (Table 2). Between these two surveys, a ~10 mm precipitation event shifted the field-average surface soil moisture from 0.347 m^3 m^{-3} to 0.388 m^3 m^{-3}, which resulted in a CV of about half and a semivariogram range parameter about ten times lower on 8 April 2019 compared to those on 5 April 2019. Previous studies have suggested that a minimum of 100 points is desirable for stable kriging interpolation (Saito and Goovaerts, 2000). Experimental semivariograms of the driest surveys (Figure 1d, 1f, 1g) and the wettest surveys (Figure 1h, 1i, 1j) shows the relatively small nugget value, which is expected for dense sampling campaigns with a separation distance between observations approaching to zero. Despite the wide gamut of semivariogram range values, we did not find any meaningful correlation of the range values with neither the mean volumetric water content nor the standard deviation of volumetric water content. Our findings suggest that the range of soil moisture spatial autocorrelation for agricultural fields at intermediate soil moisture conditions may be dictated by other factors such as soil physical properties and topography rather than soil moisture *per se*.

Delineation of management zones using soil moisture

The use of a recursive Silhouette method coupled with the FCM consistently divided the three studied fields into two soil moisture-based MZs that captured the most salient soil moisture regimes across fields with different spatial extents, soil texture, and topographic conditions (Figure 2). Previous studies at the field level using the Silhouette method in combination with clustering analysis also found that the optimal number of classes ranged between two to three classes based on multiple soil, crop, and topographic variables (Reyes et al., 2019). Maximum silhouette criterion scores were between 0.60 and 0.68 (Figure 3), indicating well-structured clusters (Kaufman and Rousseeuw, 1990) that effectively captured the distinct soil moisture regimes of each field. Fields A and B were divided into two management zones of even area, but Field C was divided into a larger wet MZ spanning nearly 76% of the field area (Table 3). This uneven distribution in Field C is attributed to the localized presence of loam soils in the lowland area of the field that resulted in drier soil moisture conditions, which as mentioned earlier, likely contributed to the high kurtosis in the soil moisture distributions of Field C.

As expected, the clustering analysis resulted in MZ with clearly distinct average soil moisture conditions and reduced intra-zone soil moisture spatial variability compared to that of the entire field (Whelan and McBratney, 2000). The dry MZs presented average soil moisture conditions about 8% lower whereas the wet MZs showed between 4.4% (Field C) to 9% (Field B) higher soil moisture compared to the average of the field. The intra-zone spatial variability quantified by the SD was substantially reduced across all three fields by about 50%. For instance, in Field C the soil moisture SD of the dry MZ was 0.026 m^3 m^{-3} and the SD of the wet zone was 0.017 m^3 m^{-3}, values that are 55% of the soil moisture SD of 0.039 m^3 m^{-3} at field level. Despite generating new more homogeneous management zones, a distinct feature of the FCM is the ability to retain information about intra-zone spatial variability based on the assigned membership grade. In contrast, hard clustering techniques (i.e. k-means) lose important information about the intra-zone spatial variability and cannot reveal less representative or transitioning areas between MZ. Although several studies have reported satisfactory results using *K*-means clustering (Arno and Rosell, 2011; Cambouris et al., 2006; Haghverdi et al., 2015), fuzzy algorithms are often regarded as a more appropriate approach to classify for continuously variable natural phenomena (Burrough, 1989).

To further investigate the controlling factors of soil moisture spatial variability in each MZ, we collected undisturbed soil samples to characterize the soil water retention properties (Figure 4). In general, wet MZs were characterized by fine-texture soils (e.g. clay loam, silty clay loam) presenting a 14% higher effective water content at saturation, 38% higher soil water content at field capacity (-10 kPa), and 207% higher soil moisture content at the permanent wilting point (-1500 kPa) compared to dry MZs characterized by coarser soil textures (e.g. sandy loam and loam soils) (Table 3). One exception occurred in Field B, in which the wetter MZ was characterized by loam soils as a result of a coarse sandy loam soil in the dry MZ characterized by even drier soil moisture conditions.

Delineation of management zones using proxy variables

Because intensive soil moisture surveys are time-consuming and labor intensive, we also analyzed MZs delineated only using the two surveys with most contrasting field-average soil moisture content and proxy variables such as elevation, clay fraction, and sand fraction. To avoid using highly correlated variables in this analysis, we conducted a pair-wise correlation between all the considered variables (Appendix A1). New MZ showed for the three fields two contrast MZ regardless of the used proxy variable (Figure 7). The Jaccard (J) index was calculated to analyze the spatial similarity between soil moisture-based MZ and proxy variables (Table 4). Delineated MZ base on only two soil moisture surveys presented the highest J similarity with values ranging from 0.60 (Field C, dry MZ) to 0.93 (Field B, wet MZ), and an average across all fields of 0.79. Thus, using two soil moisture surveys collected under contrasting field conditions arises as a plausible alternative to characterize the field soil moisture spatial variability and delineate soil moisture-based MZ using a limited number of observations. In contrast, delineated

MZ using elevation showed the lowest similarity values ranging from 0.26 (Field A, wet MZ) to 0.82 (Field C, wet MZ) with an average of 0.48. For example, on Field A located on a flat area and characterized by no changes in topography (<1% slope) presents limited relation between elevations and soil moisture MZ (Figure 7d). However, on fields with clear contrasts on elevation associated with soil type changes (e.g. Field C) elevation could be used as a proxy variable to characterize soil moisture MZ reaching similarity values of 0.82 (Figure 7f).

Another tested alternative was surface soil clay and sand fractions. In this case we did not use the soil textural class from public databases (e.g. Soil Survey Geodatabase, SSURGO), but rather the soil textural classes derived from particle size analysis using ~100 soil samples from each field (Figure 5). Resultant MZ reveals that clay and sand content were able to successfully delineate the bulk spatial pattern of soil moisture MZ with a mean similarity value of 0.61, with a minimum of 0.46 and maximum of 0.85. Based on the relation between soil hydraulic properties and soil texture by MZ previously observed (Table 3) it is expected that soil texture operated as a driven factor in soil moisture patters. Despite that, some author have found soil texture as a key variable in order to delineate MZ (Cambouris et al., 2006; Moral et al., 2010; Reyes et al., 2019), others concluded that other factors need to be considered in addition to soil texture (clay and sand percent) to delineate irrigation MZ (King et al., 2006).

During the fallow period in 2019, a survey of apparent electrical conductivity (ECa) was available to us from the owner of Field C. The ECa survey contained information for both shallow (0.5 m depth) and deep (0.7 m depth) soil layers. However, the low correlation between ECa and clay content (R^2=0.14%) and between ECa and surface volumetric water content (R^2=0.45) dissuaded us from using this single ECa survey to delineate MZ. The weak correlations in our dataset agree well with previous studies also involving observations of soil moisture on the same day of the ECa survey, in which the correlation between ECa and gravimetric water content for a single survey were also weak (R^2<0.21) (García et al., 2012). Single ECa surveys have been used to characterize the spatial variability of agricultural fields (Cambouris et al., 2006; Haghverdi et al., 2015; Johnson et al., 2003; Reyes et al., 2019), but MZ based on a single ECa survey can result in high intra-zone soil moisture spatial variability and in fragmented zones that could difficult farming management operations (Hedley and Yule, 2009b). Recent evidence shows that multiple ECa surveys are required to improve the accuracy of soil moisture estimations based on ECa surveys (García et al., 2012; Huang et al., 2017).

Soil moisture sensor location

The proposed index allowed us to define the tentative location within each MZ to install a soil moisture sensor (Figure 6). The tentative location is represented by the geographic coordinates of the center-most grid cell that best represents the MZ based on the assigned membership grade. The approach effectively ignores grid cells of high membership grade that are located at or near the edges of the MZ and centered grid cells of low and moderate membership grade. While deploying soil moisture sensors near the edge of the field can be convenient, agricultural fields usually exhibit a notorious edge-effect that could affect the representativeness of soil moisture sensors near the edges of the management zone (Carlesso et al., 2019). The edge-effect is usually caused by a combination of factors, including increased soil compaction due to excessive traffic with farming equipment, higher plant population due to overlapping of planter passes, and a different microclimate relative to the bulk of the crop (Augustin et al., 2020; Carlesso et al., 2019).

The computing of the SLI is simple, bounded by a specific range (i.e. 0 to 1), and comparable among MZs. Naturally, the optimal sensor location is largely governed by the variables used during the clustering process. In our case, the direct observation of surface soil moisture accounts for salient soil moisture spatial patterns as a result of the interaction of local environmental conditions, topographic features, soil texture, and management practices (e.g. presence of residue cover). The incorporation of alternative and readily-available factors partially related to soil moisture such us organic matter, crop yield, apparent electrical conductivity, and vegetation indices could simplify the methodology, but these factors could also introduce spatial information unrelated to soil moisture, affecting the optimal location of sensors for soil moisture monitoring. To explore the impact of additional variables, we conducted a sensitivity analysis comparing the final sensor location using the proposed method base on soil moisture against common surrogate variables (Figure 8).

The first alternative consisted of using only the soil moisture surveys with the highest and lowest mean volumetric water content in each field. The clustering analysis resulted in two well defined MZs that exhibited similar spatial patterns to those of using the full dataset (Table 4, Figure 7). As a consequence, the tentative sensor location also resulted similar geographic coordinates in each MZ. Among the three fields, the largest discrepancy was observed in the wet zone of Field C, in which the tentative sensor location using only two soil moisture surveys differed by 147 meters relative to the location found using all surveys. The lowest discrepancy was observed on the dry zone of Field A, where the two approaches differed by only 12 meters, a relatively insignificant distance within the context of large production fields. Our analysis suggests that two intensive soil moisture surveys with contrasting average soil moisture conditions could be used in place of a greater number of surveys to identify the optimal location of soil moisture sensors. A second alternative that we explored consists of delineating soil moisture MZ using observed clay and sand content. Because of the strong influence of particle size on the water holding capacity of soils, these soil physical properties are often used as a proxy for soil moisture spatial variability (Appendix A2; A3; A4). The results using soil texture showed an increased discrepancy between the tentative sensor locations ranging between 37 to 463 meters. The lowest discrepancies were observed on Field C, with values below 50 meters on both MZ, while on the other hand, Field A presented the largest discrepancies with values above ~200 meters on both MZ. As a third alternative field elevation was used to determine the sensor deployment location resulting in similar discrepancies to those observed using clay and sand content, ranging from 37 m (Field C) to 447 m (Field A). These results suggest that soil texture or elevation are able to capture the bulk shape of the soil moisture MZ, but other variables like micro-topography, soil compaction may be playing a role that can only be captured by the soil moisture observations.

Limitations of this study

One limitation of our dataset is the concentration of soil moisture observations in the top 12 cm of the soil profile. Soil profiles in the region are often characterized by well-defined soil horizons and the potentially different MZ boundaries due to sub-surface spatial variability was not account for in this study. However, intensive collection of in situ soil moisture observations can be extremely labor intensive and time-consuming. Since in the absence of a shallow water table the upper soil horizon concentrates the most extreme soil moisture dynamics, it is likely that our observations represent the predominant soil moisture regimes of the studied fields. Intensive soil moisture observations across large agricultural fields have been typically approximated in both shallow and deep soil layers using non-invasive roving instruments based on electromagnetic induction, but these instruments need to be carefully corrected to remove confounding effects of soil solutes and clay fraction that can mask soil moisture patterns.

Another limitation of our dataset is the concentration of surveys in intermediate to high field-average soil moisture conditions and the lack of surveys in drier (<0.247 $m^3 m^{-3}$) conditions. Part of the reason for the lack of drier surveys was associated with the environmental conditions during the fallow periods that only resulted in a few dry scenarios and the limited ability to take advantage of these scenarios due to the impossibility to fully insert the portable sensor in dry and hard soil conditions. The limited range of field-average soil moisture is not limited to our study. A similar study in central Italy (Brocca et al., 2007) involving the use of a portable sensor for intensive surface soil moisture monitoring in grassland plots have reported a similar field-average range, indicating that either portable soil moisture sensors are not adequate for capturing field-average conditions from air-dryness to near saturation conditions or that reaching low average soil moisture conditions over large spatial domains may require unusually long drydown periods that were not captured with these studies. Nonetheless, the observed soil moisture conditions effectively revealed the underlying spatial patterns of the studied agricultural fields caused by the complex interaction of topography, management, weather, and soil physical properties for typical soil moisture conditions. In fact, in concordance with previous studies conducted under limited temporal windows (2 to 3 months) we observed the highest soil moisture spatial variability at intermediate soil moisture conditions (0.20 to 0.25 $m^3 m^{-3}$) (Choi and Jacobs, 2011; Famiglietti et al., 2008; Tague et al., 2010), with maximum values of SD= 0.05 $m^3 m^{-3}$ similar to (Brocca et al., 2012; Tague et al., 2010). Indeed, Grayson et al. (1997) argued that soil moisture pattern is expected to be highly organized under wet conditions, whereas in drier conditions the soil moisture patterns tend to be more irregular and influenced by growing vegetation, soil properties and micro-topography.

A third limitation is that our dataset of soil moisture observations was limited to periods with no vegetation. Previous studies have shown that the impact of plant water uptake on the soil moisture spatial variability is non-negligible. The scope of our study was on the stable soil moisture spatial patterns as a result of the interplay between soil physical properties, topography, crop residue, and environmental conditions during the fallow periods. Despite not accounting for vegetation, intensive soil moisture surveys during the fallow periods revealed areas of the field with clearly distinct soil moisture regimes. Because of the strong link and control of soil texture and topography on the soil moisture spatial patterns, it is unlikely that the presence of vegetation would alter the number and total area of the delineated soil moisture-based MZ. However, the presence of an actively growing crop could impact the membership value of the grid cells, the boundaries of the MZ, and consequently on the sensors deployment location.

Conclusions

The combined use of the fuzzy-c means unsupervised clustering coupled with the silhouette cluster evaluation method allowed us to objectively identify and delineate a specific number of field MZ based on intensive surface soil moisture observations across three agricultural fields of varied soil texture and topographic conditions. Across the three studied sites, two soil moisture MZs were sufficient to capture the dominant drier and wetter soil moisture regimes mainly dictated by soil texture, elevation, and soil hydraulic properties. A sensor location index that combined the fuzzy-c means membership grade and the distance-to-edge of the MZ resulted effective to define the tentative location of soil moisture sensors within the previously delineated soil moisture-based MZ. Intensive surveys of surface soil moisture observations using a portable soil water reflectometer revealed the complex spatial patterns emerging from the interplay among weather, topography, management, and soil physical properties. The shape and area of field MZ delineated using proxy variables for soil moisture such as the percent of clay and sand showed a good agreement (i.e. high Jaccard index), with the shape and size of MZ delineated using in situ soil moisture observations alone (Figure 7), while on the contrary elevation showed a poor agreement with soil moisture-based MZ. Despite that, clay and sand content nor field elevation were able to accurately determine the soil moisture sensors deployment location compared with when soil moisture surveys observations were used. Our findings suggest that proxy variables may not accurately represent the underlying field soil moisture patterns and that, when possible, in situ soil moisture observations should be favored to guide the delineation of field MZ for improved zoning of the water management and for guiding the optimal location of a limited number of soil moisture sensors. Future studies aiming at optimizing the number and deployment location of soil moisture sensors should explore profile-level soil moisture dynamics and the impact of vegetation water uptake on the soil moisture spatial patterns. Because of the substantial amount of time and labor involved in intensive field surveys physically-based models in combination with in situ observations can span a wider range of management scenarios and soil moisture conditions. Moving towards irrigation management decisions explore the soil moisture dynamics on each delineated management zones during the crop season will allow farmers and researchers define the optimal time, frequency and rate of water applications on each MZ improving the water use efficiency of the entire system

Acknowledgments

The authors would like to acknowledge the farmers Raymond and Ryan Flickner, Justin Knopf, Garrett Kennedy, and Brian Yutzy for allowing us to conduct this research in their fields. Moreover, the authors extend special thanks to the financial support provided by the Kansas Research Experiment Station and the Kansas Corn Commission through award #A20-0027-002.

References

Adla, S., Rai, N. K., Karumanchi, S. H., Tripathi, S., Disse, M., & Pande, S. (2020). Laboratory Calibration and Performance Evaluation of Low-Cost Capacitive and Very Low-Cost Resistive Soil Moisture Sensors. Sensors, 20(2), 363. https://doi.org/10.3390/s20020363

Al-Hamdan, O. Z., & Cruise, J. F. (2010). Soil Moisture Profile Development from Surface Observations by Principle of Maximum Entropy. Journal of Hydrologic Engineering, 15(5), 327–337. https://doi.org/10.1061/(asce)he.1943-5584.0000196

Albergel, C., Udiger, C. R., Pellarin, T., Calvet, J.-C., Fritz, N., Froissard, F., Suquia, D., Petitpa, A., Piguet, B., & Martin, E. (2008). Hydrology and Earth System Sciences From near-surface to root-zone soil moisture using an exponential filter: an assessment of the method based on in-situ observations and model simulations. In Hydrol. Earth Syst. Sci (Vol. 12). www.hydrol-earth-syst-sci.net/12/1323/2008/

Allen, R. G., Pereira, L. S., Raes, D., & Smith, M. (1998). Crop evapotranspiration-Guidelines for computing crop water requirements. Guidelines for Computing Crop Water Requirements-FAO Irrigation and Drainage Paper 56. FAO Rome, 300(9), 109.

Andales, A. A., Bauder, T. A., & Arabi, M. (2015). A Mobile Irrigation Water Management System Using a Collaborative GIS and Weather Station Networks (pp. 53–84). https://doi.org/10.2134/advagricsystmodel5.c3

Satorra, J. A., Casasnovas, J. A. M., Ribes-Dasi, M., & Polo, J. R. R. (2011). Clustering of grape yield maps to delineate site-specific management zones. *Spanish Journal of Agricultural Research*, (3), 721-729..

Augustin, K., Kuhwald, M., Brunotte, J., & Duttmann, R. (2020). Wheel Load and Wheel Pass Frequency as Indicators for Soil Compaction Risk: A Four-Year Analysis of Traffic Intensity at Field Scale. Geosciences, 10(8), 292. https://doi.org/10.3390/geosciences10080292

Barker, J. B., Franz, T. E., Heeren, D. M., Neale, C. M. U., & Luck, J. D. (2017). Soil water content monitoring for irrigation management: A geostatistical analysis. Agricultural Water Management, 188, 36–49. https://doi.org/10.1016/j.agwat.2017.03.024

Basso, B., Bertocco, M., Sartori, L., & Martin, E. C. (2007). Analyzing the effects of climate variability on spatial pattern of yield in a maize-wheat-soybean rotation. European Journal of Agronomy, 26(2), 82–91. https://doi.org/10.1016/j.eja.2006.08.008

Bezdek, J. C. (1981). Objective function clustering. In Pattern recognition with fuzzy objective function algorithms (pp. 43-93). Springer, Boston, MA.

Bittelli, M., & Flury, M. (2009). Errors in Water Retention Curves Determined with Pressure Plates. Soil Science Society of America Journal, 73(5), 1453–1460. https://doi.org/10.2136/sssaj2008.0082

Boluwade, A., Chandra Madramootoo, C., & Yari, A. (2015). Application of Unsupervised Clustering Techniques for Management Zone Delineation: Case Study of Variable Rate Irrigation in Southern Alberta, Canada. Journal of Irrigation and Drainage Engineering, 142(1), 05015007. https://doi.org/10.1061/(ASCE)IR.1943-4774.0000936

Boydell, B., & Mcbratney, A. B. (2002). Identifying Potential Within-Field Management Zones from Cotton-Yield Estimates. Precision Agriculture 3(1), 9-23.

Brocca, L., Morbidelli, R., Melone, F., & Moramarco, T. (2007). Soil moisture spatial variability in experimental areas of central Italy. Journal of Hydrology, 333(2–4), 356–373. https://doi.org/10.1016/j.jhydrol.2006.09.004

Brocca, L., Tullo, T., Melone, F., Moramarco, T., & Morbidelli, R. (2012). Catchment scale soil moisture spatial-temporal variability. Journal of Hydrology, 422–423, 63–75. https://doi.org/10.1016/j.jhydrol.2011.12.039

Burrough, P. A. (1989). Fuzzy mathematical methods for soil survey and land evaluation. Journal of Soil Science, 40(3), 477–492.

BURROUGH, P. A. (1989). Fuzzy mathematical methods for soil survey and land evaluation. Journal of Soil Science, 40(3), 477–492. https://doi.org/10.1111/j.1365-2389.1989.tb01290.x

Calvet, J. C., & Noilhan, J. (2000). From near-surface to root-zone soil moisture using year-round data. Journal of Hydrometeorology, 1(5), 393–411. https://doi.org/10.1175/1525-7541(2000)001<0393:FNSTRZ>2.0.CO;2

Cambardella, C. A., Moorman, T. B., Novak, J. M., Parkin, T. B., Karlen, D. L., Turco, R. F., & Konopka, A. E. (1994). Field-Scale Variability of Soil Properties in Central Iowa Soils. Soil Science Society of America Journal, 58(5), 1501–1511. https://doi.org/10.2136/sssaj1994.03615995005800050033x

Cambouris, A. N., Nolin, M. C., Zebarth, B. J., & Laverdisre, M. R. (2006). Soil Management Zones Delineated by Electrical Conductivity to Characterize Spatial and Temporal Variations in Potato Yield and in Soil Properties. In Amer J of Potato Res (Vol. 83).

Carlesso, L., Beadle, A., Cook, S. M., Evans, J., Hartwell, G., Ritz, K., Sparkes, D., Wu, L., & Murray, P. J. (2019). Soil compaction effects on litter decomposition in an arable field: Implications for management of crop residues and headlands. Applied Soil Ecology, 134, 31–37. https://doi.org/10.1016/j.apsoil.2018.10.004

Ceballos, A., Scipal, K., Wagner, W., & Martínez-Fernández, J. (2005). Validation of ERS scatterometer-derived soil moisture data in the central part of the Duero Basin, Spain. Hydrological Processes, 19(8), 1549–1566. https://doi.org/10.1002/hyp.5585

Choi, M., & Jacobs, J. M. (2011). Spatial soil moisture scaling structure during Soil Moisture Experiment 2005. Hydrological Processes, 25(6), 926–932. https://doi.org/10.1002/hyp.7877

Cococcioni, M. (2020). ffcmw: The Fastest Fuzzy C-Means in the West! (https://www.mathworks.com/matlabcentral/fileexchange/53029-ffcmw-the-fastest-fuzzy-c-means-in-the-west), MATLAB Central File Exchange. Retrieved February 14, 2020. MATLAB Central File Exchange. https://www.mathworks.com/matlabcentral/fileexchange/53029-ffcmw-the-fastest-fuzzy-c-means-in-the-west

Dieter, C. A., Maupin, M. A., Caldwell, R. R., Harris, M. A., Ivahnenko, T. I., Lovelace, J. K., Barber, N. L., & Linsey, K. S. (2018). Estimated use of water in the United States in 2015. U.S. Geological Survey Circular. https://doi.org/https://doi.org/10.3133/cir1441. [Supersedes USGS Open-File Report 2017–1131.]

Ding, J., & Chandra, R. (2019). Estimating Soil Moisture and Electrical Conductivity Using Wi-Fi. In Proc. ACM MobiCom.

Dobriyal, P., Qureshi, A., Badola, R., & Hussain, S. A. (2012). A review of the methods available for estimating soil moisture and its implications for water resource management. In Journal of Hydrology (Vols. 458–459, pp. 110–117). Elsevier. https://doi.org/10.1016/j.jhydrol.2012.06.021

Entekhabi, D., Njoku, E. G., O'Neill, P. E., Kellogg, K. H., Crow, W. T., Edelstein, W. N., Entin, J. K., Goodman, S. D., Jackson, T. J., Johnson, J., Kimball, J., Piepmeier, J. R., Koster, R. D., Martin, N., McDonald, K. C., Moghaddam, M., Moran, S., Reichle, R., Shi, J. C., … Van Zyl, J. (2010). The soil moisture active passive (SMAP) mission. Proceedings of the IEEE, 98(5), 704–716. https://doi.org/10.1109/JPROC.2010.2043918

Er-Raki, S., Chehbouni, A., Boulet, G., & Williams, D. G. (2010). Using the dual approach of FAO-56 for partitioning ET into soil and plant components for olive orchards in a semi-arid region. Agricultural Water Management, 97(11), 1769–1778. https://doi.org/10.1016/j.agwat.2010.06.009

Evans, R. G., LaRue, J., Stone, K. C., & King, B. A. (2013). Adoption of site-specific variable rate sprinkler irrigation systems. In Irrigation Science (Vol. 31, Issue 4, pp. 871–887). https://doi.org/10.1007/s00271-012-0365-x

Falkenmark, M., Fox, P., Persson, G., & Rockström, J. (2001). Water Harvesting for Upgrading of Rainfed Agriculture: Problem Analysis and Research Needs, Stockholm International Water Institute. SIWI Report II.

Famiglietti, J., Rudnicki, J. W., & Rodell, M. (1998). Variability in surface moisture content along a hillslope transect: Rattlesnake Hill, Texas. Journal of Hydrology, 210(1–4), 259–281. https://doi.org/10.1016/S0022-1694(98)00187-5

Famiglietti, J S, Devereaux, J. A., Laymon, C. A., Tsegaye, T., Houser, P. R., Jackson, T. J., Graham, S. T., Rodell, M., & Van Oevelen, P. J. (1999). Ground-based investigation of soil moisture variability within remote sensing footprints during the Southern Great Plains 1997 (SGP97) Hydrology Experiment. Water Resources Research, 35(6), 1839-1851.

Famiglietti, James S., Ryu, D., Berg, A. A., Rodell, M., & Jackson, T. J. (2008). Field observations of soil moisture variability across scales. Water Resources Research, 44(1). https://doi.org/10.1029/2006WR005804

FAO. (2021). Food and Agriculture Organization of the United Natios Statistics Division. FAO. http://www.fao.org/land-water/world-water-day-2021/watergovernance/irrigation-reform/en/

Ford, T. W., Harris, E., & Quiring, S. M. (2014). Estimating root zone soil moisture using near-surface observations from SMOS. Hydrology and Earth System Sciences, 18(1), 139–154. https://doi.org/10.5194/hess-18-139-2014

Fraisse, C. W., Sudduth, K. A., & Kitchen, N. R. (2001). Ddelineation of site-specific management zones by unsupervised classification of topographic attributes and soil electrical conductivity. In American Society of Agricultural Engineers (Vol. 155, Issue 1).

García, G. M., Vanderlinden, K., Pachepsky, Y., Cervera, J. V. G., & Pérez, A. J. E. (2012). Estimating Topsoil Water Content of Clay Soils With Data From Time-Lapse Electrical Conductivity Surveys. Soil Science, 177(6), 369–376. https://doi.org/10.1097/SS.0b013e31824eda57

Gavlak, R., Horneck, D., Miller, R. O., & Kotuby-Amacher, J. (2003). Soil, plant and water reference methods for the western region. WCC-103 Publication, Fort Collins, CO.

Grinsted, A., Moore, J. C., & Jevrejeva, S. (2004). Nonlinear Processes in Geophysics Application of the cross wavelet transform and wavelet coherence to geophysical time series (Vol. 11). http://www.pol.ac.uk/home/research/waveletcoherence/

Haghverdi, A., Leib, B. G., Washington-Allen, R. A., Ayers, P. D., & Buschermohle, M. J. (2015). Perspectives on delineating management zones for variable rate irrigation. Computers and Electronics in Agriculture, 117, 154–167. https://doi.org/10.1016/j.compag.2015.06.019

Hassanli, A. M., Ebrahimizadeh, M. A., & Beecham, S. (2009). The effects of irrigation methods with effluent and irrigation scheduling on water use efficiency and corn yields in an arid region. Agricultural Water Management, 96(1), 93–99. https://doi.org/10.1016/j.agwat.2008.07.004

Hedley, C. B., & Yule, I. J. (2009a). A method for spatial prediction of daily soil water status for precise irrigation scheduling. Agricultural Water Management, 96(12), 1737–1745. https://doi.org/10.1016/j.agwat.2009.07.009

Hedley, C. B., & Yule, I. J. (2009b). A method for spatial prediction of daily soil water status for precise irrigation scheduling. Agricultural Water Management, 96(12), 1737–1745. https://doi.org/10.1016/j.agwat.2009.07.009

Hedley, C., Ekanayake, J., & Roudier, P. (2012). Wireless soil moisture sensor networks for precision irrigation scheduling. Workshop Abstracts, Advanced Nutrient Management: Gains from the Past-Goals for the Future., 85. www.precisionirrigation.co.nz

Hedley, C., Ekanayake, J., Roudier, P., Road, R., Street, G., & Zealand, N. (2009). Wireless Soil Moisture Sensor Networks for Precision. 1–10.

Hengl, T. (2006). Finding the right pixel size. Computers and Geosciences, 32(9), 1283–1298. https://doi.org/10.1016/j.cageo.2005.11.008

Huang, J., Scudiero, E., Clary, W., Corwin, D. L., & Triantafilis, J. (2017). Time-lapse monitoring of soil water content using electromagnetic conductivity imaging. Soil Use and Management, 33(2), 191–204. https://doi.org/10.1111/sum.12261

Hupet, F., & Vanclooster, M. (2002). Intraseasonal dynamics of soil moisture variability within a small agricultural maize cropped field. Journal of Hydrology, 261(1–4), 86–101. https://doi.org/10.1016/S0022-1694(02)00016-1

Irmak, S., Burgert, M. J., Yang, H. S., Cassman, K. G., Walters, D. T., Rathje, W. R., Payero, J. O., Grassini, P., Kuzila, M. S., Brunkhorst, K. J., Eisenhauer, D. E., Kranz, W. L., Vandewalle, B., Rees, J. M., Zoubek, G. L., Shapiro, C. A., & Teichmeier, G. J. (2012). Large-scale on-farm implementation of soil moisture-based irrigation management strategies for increasing maize water productivity. 55(3), 881–894.

Johnson, C. K., Mortensen, D. A., Wienhold, B. J., Shanahan, J. F., & Doran, J. W. (2003). Site-Specific Management Zones Based on Soil Electrical Conductivity in a Semiarid Cropping System. Agronomy Journal, 95(2), 303–315. https://doi.org/10.2134/agronj2003.3030

Kansas Mesonet. (2021). Kansas Mesonet, 2021. Data, Kansas Mesonet Historical. Accessed 26 January 2021,Http://Climate.k-State.Edu/Precip/County/.

Kaufman, L., & Rousseeuw, P. J. (1990). Finding groups in data: an introduction to cluster analysis (Vol. 344). John Wiley & Sons.

Keating, B. A., Carberry, P. S., Hammer, G. L., Probert, M. E., Robertson, M. J., Holzworth, D., Huth, N. I., Hargreaves, J. N., Meinke, H., Hochman, Z., & McLean, G. (2003). An overview of APSIM, a model designed for farming systems simulation. European Journal of Agronomy, 18(3–4), 267–288.

Kebede, H., Fisher, D. K., Sui, R., & Reddy, K. N. (2014). Irrigation Methods and Scheduling in the Delta Region of Mississippi: Current Status and Strategies to Improve Irrigation Efficiency. American Journal of Plant Sciences, 05(20), 2917–2928. https://doi.org/10.4236/ajps.2014.520307

King, B. A., Stark, J. C., & Wall, R. W. (2006). Comparison of site-specific and conventional uniform irrigation management for potatoes. Applied Engineering in Agriculture, 22(5), 677-688.

Kukal, M. S., Irmak, S., & Sharma, K. (2020). Development and application of a performance and operational feasibility guide to facilitate adoption of soil moisture sensors. Sustainability (Switzerland), 12(1). https://doi.org/10.3390/su12010321

Ledieu, J., De Ridder, P., De Clerck, P., & Dautrebande, S. (1986). A method of measuring soil moisture by time-domain reflectometry. Journal of Hydrology, 88(3–4), 319–328. https://doi.org/10.1016/0022-1694(86)90097-1

MacQueen, J. (1967). Some methods for classification and analysis of multivariate observations. Proceedings of the Fifth Berkeley Symposium on Mathematical Statistics and Probability, 1(14).

Mahmood, R., Littell, A., Hubbard, K. G., & You, J. (2012). Observed data-based assessment of relationships among soil moisture at various depths, precipitation, and temperature. Applied Geography, 34, 255–264. https://doi.org/10.1016/j.apgeog.2011.11.009

Maurer, C. R., Qi, R., & Raghavan, V. (2003). A linear time algorithm for computing exact Euclidean distance transforms of binary images in arbitrary dimensions. IEEE Transactions on Pattern Analysis and Machine Intelligence, 25(2), 265–270. https://doi.org/10.1109/TPAMI.2003.1177156

McGuire, V. (2012). Water-Level and Storage Changes in the High Plains Aquifer, Predevelopment to 2011 and 2009–11. Publications of the US Geological Survey. https://digitalcommons.unl.edu/usgspubs/123

Mishra, V., Lee Ellenburg, W., Markert, K. N., Limaye, A. S., & Pingale, S. (2020). Performance evaluation of soil moisture profile estimation through entropy-based and exponential filter models Performance evaluation of soil moisture profile estimation through entropy-based and exponential filter models Performance evaluation of soil mo. Hydrological Sciences Journal, 65(6), 1036–1048. https://doi.org/10.1080/02626667.2020.1730846

Moral, F. J., Terrón, J. M., & Silva, J. R. M. da. (2010). Delineation of management zones using mobile measurements of soil apparent electrical conductivity and multivariate geostatistical techniques. Soil and Tillage Research, 106(2), 335–343. https://doi.org/10.1016/j.still.2009.12.002

Nash, J. E., & Sutcliffe, J. V. (1970). River flow forecasting through conceptual models part I - A discussion of principles. Journal of Hydrology, 10(3), 282–290. https://doi.org/10.1016/0022-1694(70)90255-6

NASS, U. (2014). Farm and Ranch Irrigation Survey (2013). Farm and Ranch Irrigation Survey (2013); National Agricultural Statistics Service, Ed.; United States Department of Agriculture:, 3, 266.

NASS, U. (2018). Irrigation and Water Management Results from the 2018 Irrigation and Water Management Survey. USDA NASS 2018 Irrigation and Water Management Survey (2017 Census of Agriculture). www.nass.usda.gov/AgCensus

Oldoni, H., & Bassoi, L. H. (2016). Delineation of irrigation management zones in a Quartzipsamment of the Brazilian semiarid region. Pesquisa Agropecuaria Brasileira, 51(9), 1283–1294. https://doi.org/10.1590/S0100-204X2016000900028

Payero, J. O., Tarkalson, D. D., Irmak, S., Davison, D., & Petersen, J. L. (2008). Effect of irrigation amounts applied with subsurface drip irrigation on corn evapotranspiration, yield, water use efficiency, and dry matter production in a semiarid climate. Agricultural Water Management, 95(8), 895–908. https://doi.org/10.1016/j.agwat.2008.02.015

Peralta, N. R., Costa, J. L., Balzarini, M., Castro Franco, M., Córdoba, M., & Bullock, D. (2015). Delineation of management zones to improve nitrogen management of wheat. Computers and Electronics in Agriculture, 110, 103–113. https://doi.org/10.1016/j.compag.2014.10.017

Pereira, L. S. (2017). Water, Agriculture and Food: Challenges and Issues. Water Resources Management, 31(10), 2985–2999. https://doi.org/10.1007/s11269-017-1664-z

Peterson, A. M., Helgason, W. D., & Ireson, A. M. (2016). Estimating field-scale root zone soil moisture using the cosmic-ray neutron probe. Hydrology and Earth System Sciences, 20(4), 1373–1385. https://doi.org/10.5194/hess-20-1373-2016

Reyes, J., Wendroth, O., Matocha, C., & Zhu, J. (2019). Delineating site-specific management zones and evaluating soil water temporal dynamics in a farmer's field in Kentucky. Vadose Zone Journal, 18(1). https://doi.org/10.2136/vzj2018.07.0143

Rousseeuw, P. J. (1987). Silhouettes: A graphical aid to the interpretation and validation of cluster analysis. Journal of Computational and Applied Mathematics, 20(C), 53–65. https://doi.org/10.1016/0377-0427(87)90125-7

Sadler, E. J., Evans, R. G., Stone, K. C., & Camp, C. R. (2005). Opportunities for conservation with precision irrigation. Soil Water Conservation, 60, 371–379. https://pubag.nal.usda.gov/download/18977/PDF

Saito, H., & Goovaerts, P. (2000). Geostatistical interpolation of positively skewed and censored data in a dioxin-contaminated site. Environmental Science and Technology, 34(19), 4228–4235. https://doi.org/10.1021/es991450y

Saito, H., & Goovaerts, P. (2003). Selective remediation of contaminated sites using a two-level multiphase strategy and geostatistics. Environmental Science and Technology, 37(9), 1912–1918. https://doi.org/10.1021/es020737j

Schepers, A. R., Shanahan, J. F., Liebig, M. A., Schepers, J. S., Johnson, S. H., & Luchiari, A. (2004). Appropriateness of Management Zones for Characterizing Spatial Variability of Soil Properties and Irrigated Corn Yields across Years. Agronomy Journal, 96(1), 195–203. https://doi.org/10.2134/AGRONJ2004.1950

Schindler, U. (1980). Ein schnellverfahren zur messung der wasserleitfähigkeit im teilgesättigten boden an stechzylinderproben.

Seyfried, M. S., & Grant, L. E. (2007). Temperature Effects on Soil Dielectric Properties Measured at 50 MHz. Vadose Zone Journal, 6(4), 759–765. https://doi.org/10.2136/vzj2006.0188

Šimůnek, J., van Genuchten, M. T., & Šejna, M. (2008). Development and applications of the HYDRUS and STANMOD software packages and related codes. Vadose Zone Journal, 7(2), 587–600.

Soil Survey Staff. (2020). Soil Survey Staff, Natural Resources Conservation Service, United States Department of Agriculture. https://websoilsurvey.sc.egov.usda.gov/. Accessed

Spencer, G. D., Falconer, L. L., Iii, H. C. P., Bryant, C. J., Atwill, R. L., Henry, W. B., Krutz, L. J., Henry, C. G., & Larson, E. J. (2019). Crop Management Irrigation Water Management Technologies for Furrow-Irrigated Corn that Decrease Water Use and Improve Yield and On-Farm Profitability. https://doi.org/10.2134/cftm2018.12.0100

Spencer, G. D., Krutz, L. J., Falconer, L. L., Henry, W. B., Henry, C. G., Larson, E. J., Pringle III, H. C., Bryant, C. J., & Atwill, R. L. (2019). Irrigation Water Management Technologies for Furrow-Irrigated Corn that Decrease Water Use and Improve Yield and On-Farm Profitability. Crop Forage Turfgrass Manage.

Survey, U. S. G. (2017). 1/3rd arc-second Digital Elevation Models (DEMs) - USGS National Map 3DEP Downloadable Data Collection. https://www.sciencebase.gov/catalog/item/4f70aa9fe4b058caae3f8de5

Tague, C., Band, L., Kenworthy, S., & Tenebaum, D. (2010). Plot- and watershed-scale soil moisture variability in a humid Piedmont watershed. Water Resources Research, 46(12). https://doi.org/10.1029/2009WR008078

Thorp, K. R., Hunsaker, D. J., Bronson, K. F., Andrade-Sanchez, P., & Barnes, E. M. (2017). Cotton Irrigation Scheduling Using a Crop Growth Model and FAO-56 Methods: Field and Simulation Studies. Transactions of the ASABE, 60(6), 2023–2039. https://doi.org/10.13031/trans.12323

Vachaud, G., Passerat de Silans, A., Balabanis, P., & Vauclin, M. (1985). Temporal stability of spatially measured soil water probability density function 1. Soil Science Society of America Journal, 49(4), 822–828. https://dl.sciencesocieties.org/publications/sssaj/abstracts/49/4/SS0490040822

van Genuchten, M. T. (1980). A Closed-form Equation for Predicting the Hydraulic Conductivity of Unsaturated Soils. Soil Science Society of America Journal, 44(5), 892–898. https://doi.org/10.2136/sssaj1980.03615995004400050002x

Wagner, W., Lemoine, G., & Rott, H. (1999). A method for estimating soil moisture from ERS Scatterometer and soil data. Remote Sensing of Environment, 70(2), 191–207. https://doi.org/10.1016/S0034-4257(99)00036-X

Wang, T., Franz, T. E., You, J., Shulski, M. D., & Ray, C. (2017). Evaluating controls of soil properties and climatic conditions on the use of an exponential filter for converting near surface to root zone soil moisture contents. Journal of Hydrology, 548, 683–696. https://doi.org/10.1016/j.jhydrol.2017.03.055

Weaver, J. E., & Darland, R. W. (1949). Soil-root relationships of certain native grasses in various soil types. Wiley on Behalf of the Ecological Society of America - Ecological Monographs, 19(4), 303–338.

Western, A., & Grayson, R. (2000). Soil Moisture and Runoff Processes at Tarrawarra. Spatial Patterns in Catchment Hydrology: Observations and Modelling, 209–246.

Western, A. W., Grayson, R. B., Blöschl, G., & Wilson, D. J. (2003). Spatial variability of soil moisture and its implications for scaling. In Scaling methods in soil physics (pp. 119–142).

Whelan, B. M., & McBratney, A. B. (2000). The "null hypothesis" of precision agriculture management. Precision Agriculture, 2(3), 265–279. https://doi.org/10.1023/A:1011838806489

Wind, G. P. (1966). Capillary conductivity data estimated by a simple method. R.E. Rijtema and H. Wassink (Ed.) Water in the Unsaturated Zone: Proc. UNESCO/IASH Symp., Wageningen, the Netherlands, 80, 181–191.

Yan, L., Shi, Z., Li, F., & Li, H. Y. (2007). Delineation of site-specific management zones using fuzzy clustering analysis in a coastal saline land. Computers and Electronics in Agriculture, 56(2), 174–186. https://doi.org/10.1016/j.compag.2007.01.013

Yari, A., Madramootoo, C. A., Woods, S. A., Adamchuk, V. I., & Huang, H.-H. (2017). Assessment of Field Spatial and Temporal Variabilities to Delineate Site-Specific Management Zones for Variable-Rate Irrigation. Journal of Irrigation and Drainage Engineering, 143(9), 04017037. https://doi.org/10.1061/(ASCE)IR.1943-4774.0001222

Zhao, W., Li, J., Yang, R., & Li, Y. (2018). Determining placement criteria of moisture sensors through temporal stability analysis of soil water contents for a variable rate irrigation system. Precision Agriculture, 19, 648–665. https://doi.org/10.1007/s11119-017-9545-2

Table 0.1. Field area, approximate sampling grid size, number of soil moisture surveys, and total number of surface (0-12 cm) soil moisture observations for each field.

Field†	Field area	Sampling grid size‡	Number of surveys	Total number of observations
	ha	m		
A	28	25 x 25	6	2575
B	58	80 x 80	3	873
C	22	50 x 50	7	1211

† Letters were assigned to fields to protect the identity and location of the producers
‡ Sampling grid size was defined base on field area, available workforce, and a minimum number of samples required to interpolate soil moisture using a 5 m grid resolution.

Table 0.2. Statistical properties of the soil moisture surveys collected during the fallow periods at the three agricultural fields.

Field	Date	N	Mean	SD	CV	Min-Max	Skew.	Kurt.	SV†	Range‡	NSR¶
			$m^3 m^{-3}$	$m^3 m^{-3}$	%	$m^3 m^{-3}$				m	
A	9-May-17*	402	0.317	0.038	12.1	0.222 - 0.439	0.18	2.96	S	232	26.6
A	16-May-17*	286	0.310	0.037	11.8	0.205 - 0.410	-0.10	2.92	S	130	18.3
A	23-May-17	356	0.365	0.029	7.9	0.295 - 0.483	0.31	3.34	S	192	4.09
A	30-May-17*	424	0.321	0.038	11.8	0.224 - 0.453	0.00	2.94	S	168	10.1
A	5-Jul-17	594	0.265	0.048	18.3	0.159 - 0.442	0.68	3.79	E	242	13.3
A	7-Jul-17*	513	0.261	0.044	16.8	0.133 - 0.392	0.16	3.11	E	134	6.19
B	5-Nov-18*	422	0.283	0.037	13.0	0.179 - 0.386	0.04	2.61	E	153	22.4
B	16-Nov-18*	307	0.314	0.031	9.7	0.234 - 0.409	-0.08	2.67	E	227	76.0
B	5-Jun-19*	177	0.247	0.050	20.3	0.123 - 0.360	-0.06	2.48	S	142	2.01
C	1-Apr-19	208	0.362	0.041	11.4	0.220 - 0.448	-1.22	4.54	E	325	48.0
C	5-Apr-19	215	0.347	0.046	13.2	0.177 - 0.436	-0.72	3.16	E	792	64.6
C	8-Apr-19	161	0.388	0.026	6.8	0.264 - 0.459	-1.17	6.78	E	77	6.24
C	17-Apr-19	166	0.331	0.039	11.9	0.213 - 0.465	-0.48	3.97	E	280	37.5
C	22-Apr-19	270	0.323	0.041	12.8	0.177 - 0.442	-0.35	3.14	E	144	23.7
C	3-May-19	69	0.384	0.037	9.5	0.255 - 0.440	-1.50	5.47	S	-	0.17
C	27-Jun-19*	122	0.340	0.042	12.3	0.259 - 0.437	0.09	2.29	E	191	10.9

*Surveys statistically normal according to the Shapiro-Wilk test using a 5% significance level.

†Semivariogram model that best fitted (lowest RMSE) the empirical semivariogram (G=Gaussian, S=Spherical, E=Exponential).

‡Range parameter of the selected semivariogram model. The survey on 3 May 2019 only had 69 observations and the semivariogram was ill-conditioned, with a range value far exceeding the size of the field.

¶Nugget to Sill ratio of the selected semivariogram model.

Table 0.3. Area, predominant soil textural class, mean volumetric water content ($\boldsymbol{\theta_{mean}}$), clay and sand fractions, volumetric water content at saturation ($\boldsymbol{\theta_{sat}}$), field capacity ($\boldsymbol{\theta_{fc}}$, -10 kPa), permanent wilting point ($\boldsymbol{\theta_{wp}}$, -1500 kPa), and plant available water (PAW) for each management zone.

Field	Zone	Field area	Textural class†	θ_{mean}	Clay‡	Sand‡	θ_{sat}¶	θ_{fc}¶	θ_{wp}¶	PAW
		ha (%)		$m^3\ m^{-3}$	%	%	$m^3\ m^{-3}$	$m^3\ m^{-3}$	$m^3\ m^{-3}$	$m^3\ m^{-3}$
A	Dry	12.7 (45)	Loam (78 %)	0.279	20	34	0.409	0.310	0.081	0.229
A	Wet	15.1 (54)	C loam (37%)	0.328	27	26	0.482	0.363	0.197	0.166
B	Dry	28.6 (49)	S loam (50%)	0.265	16	51	0.388	0.276	0.076	0.200
B	Wet	30.0 (51)	Loam (86%)	0.306	18	44	0.447	0.391	0.146	0.245
C	Dry	5.3 (24)	Loam (56%)	0.328	24	30	0.392	0.235	0.112	0.123
C	Wet	17.1 (76)	Si C loam (41%)	0.371	29	19	0.426	0.368	0.210	0.158

†Predominant soil textural class for each management zone. Values between parenthesis indicate the percentage of the area of the management zone occupied by the predominant soil texture average. C= Clay, S= Sandy, and Si= Silty.

‡Average clay and sand fractions using all sampling points within the management zone.

¶Values of θ_{sat}, θ_{fc}, and θ_{wp} were determined in laboratory conditions from a limited number of undisturbed soil samples collected in each management zone.

Table 0.4. Jaccard index values used to compare the spatial similarity between soil moisture-based MZ with delineated MZ using proxy variables: only two soil moisture surveys, field elevation and soil clay and sand fraction.

Field	Zone	Two Surveys	Field Elevation	Clay and Sand
A	Dry	0.73	0.30	0.63
A	Wet	0.73	0.26	0.66
B	Dry	0.92	0.41	0.46
B	Wet	0.93	0.54	0.58
C	Dry	0.60	0.55	0.50
C	Wet	0.84	0.82	0.85

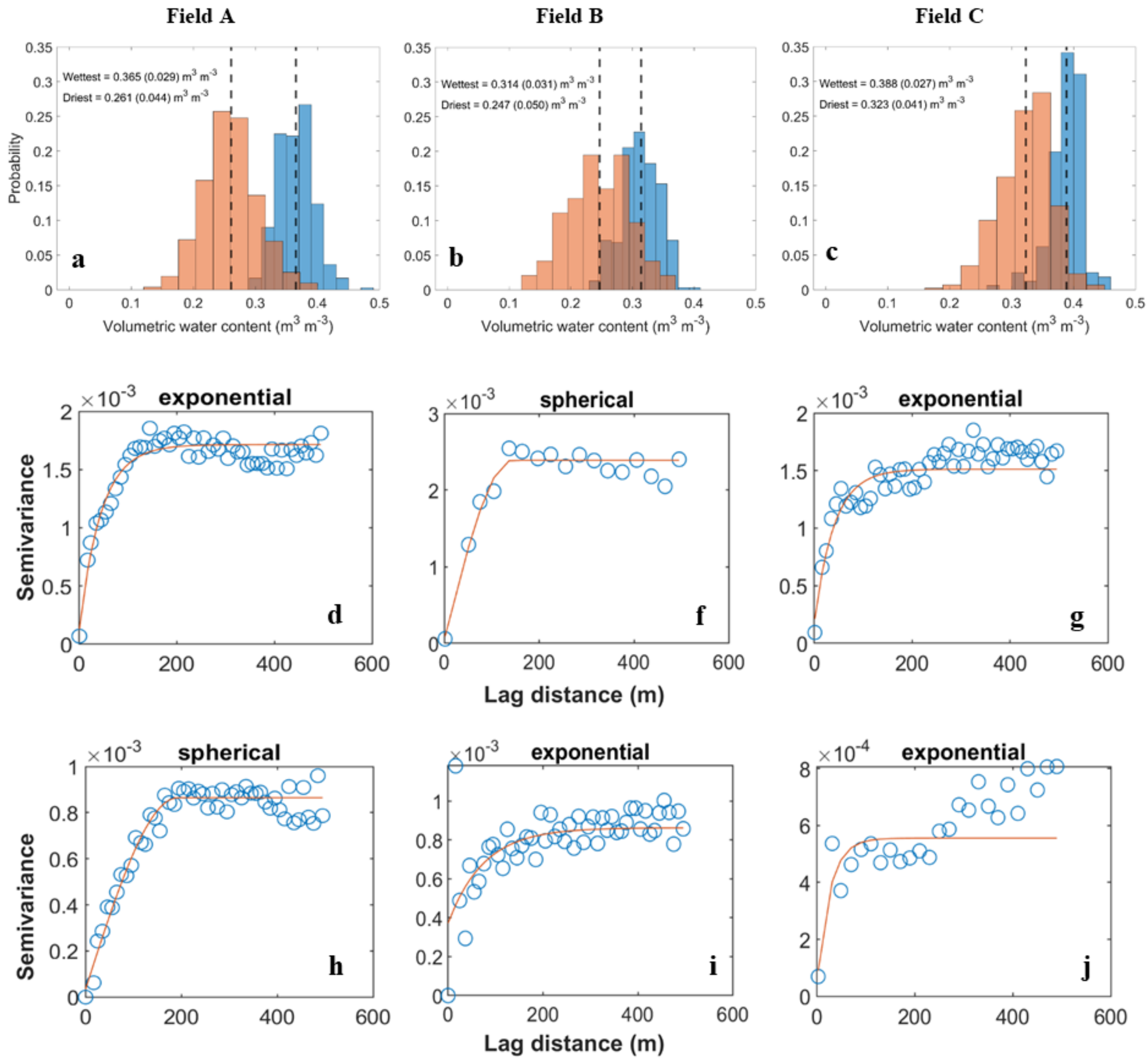

Figure 0.1. Histograms (a-c) and fitted semivariogram models of the driest (d-g) and wettest (h-j) soil moisture surveys in each field. Mean (±1 SD) values are provided for each survey and the mean soil moisture of each survey is also indicated with a vertical dashed line.

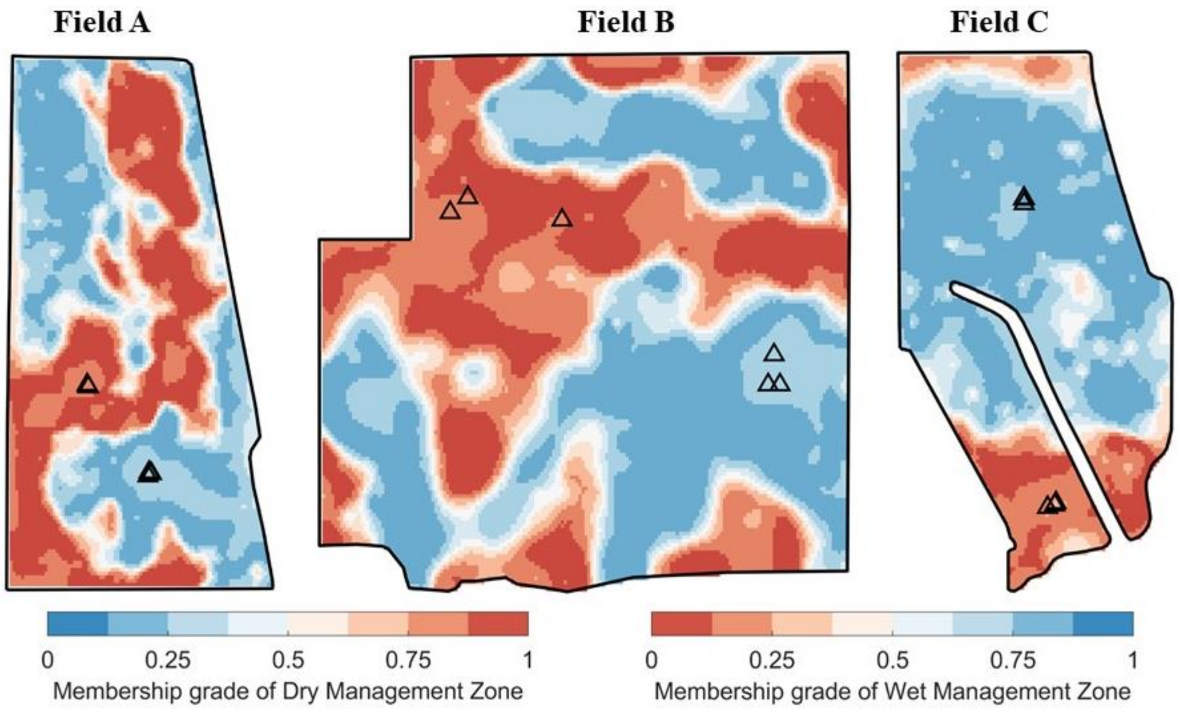

Figure 0.2. Delineated MZ using the FCM clustering technique based on surface (0-12 cm) soil moisture observations for each field. The membership grade (1 is highest and 0 is lowest membership) indicates the degree of belonging of each grid cell to a specific management zone. Triangle markers represent the location of undisturbed soil samples for characterizing the soil water retention properties of each management zone.

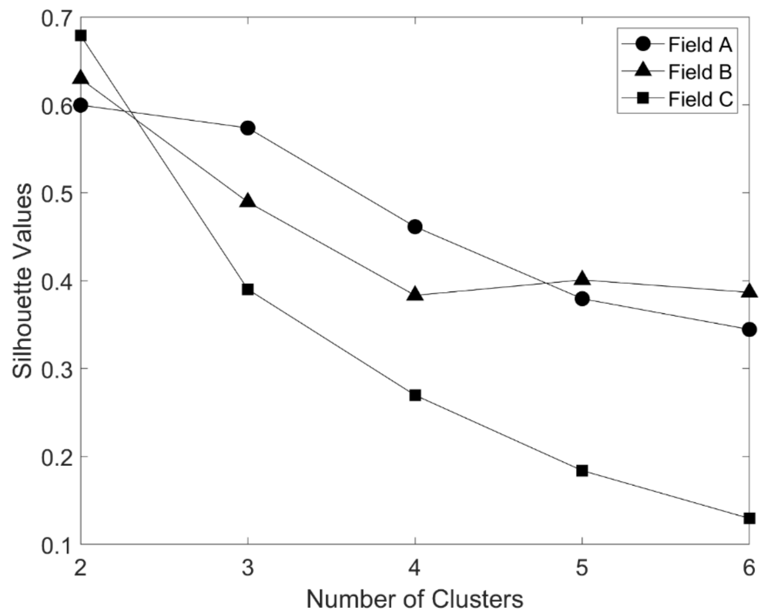

Figure 0.3. Silhouette values used to define the optimum number of management zones at each field. Silhouette values range between -1 and 1, where the highest value indicates the optimal number of clusters.

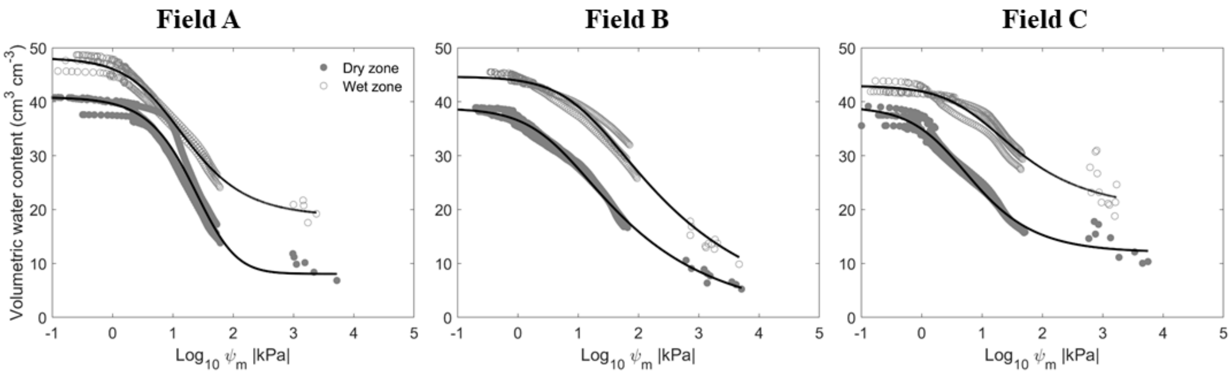

Figure 0.4. Soil water retention curves for each management zone. Filled circles correspond to the dry management zone and hollow circles to the wet management zones.

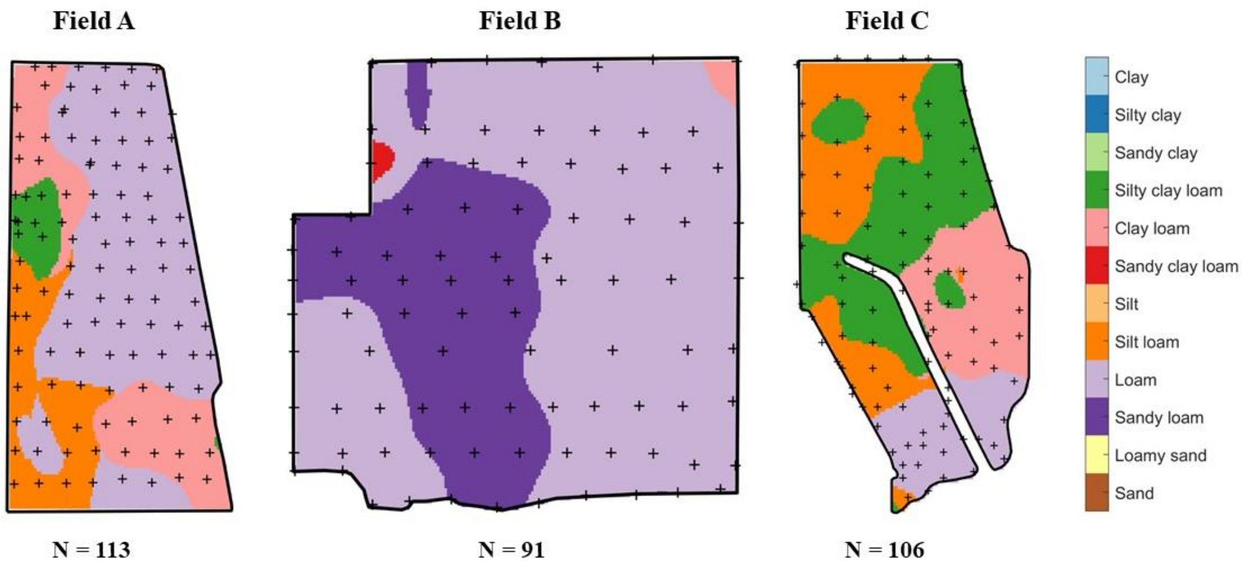

Figure 0.5. Soil textural classes of the top 12 cm. Black crosses (+) represent soil sampling location across each field. In total our study spanned five major soil textural classes (excluding a single observation of sandy clay loam soils).

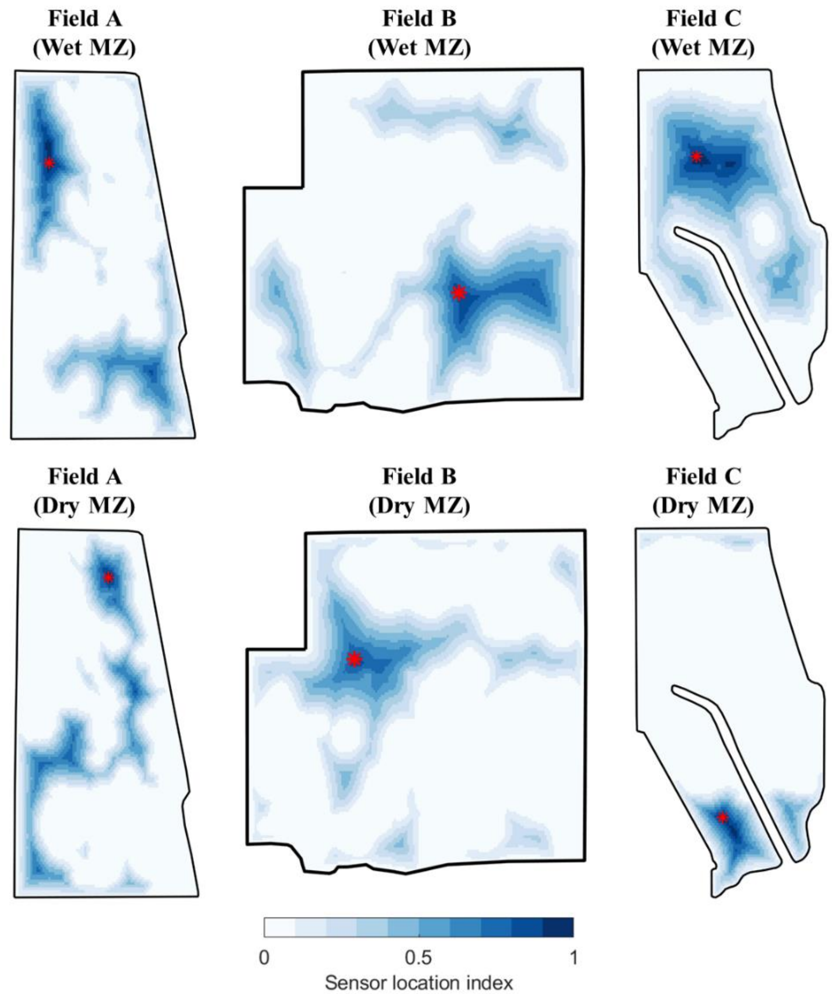

Figure 0.6. Optimal locations for installing one soil moisture sensor per delineated management zone based on the sensor location index (SLI). The SLI ranges from 0 to 1, where high values represent centralized grid cells within each management zone with high membership grade.

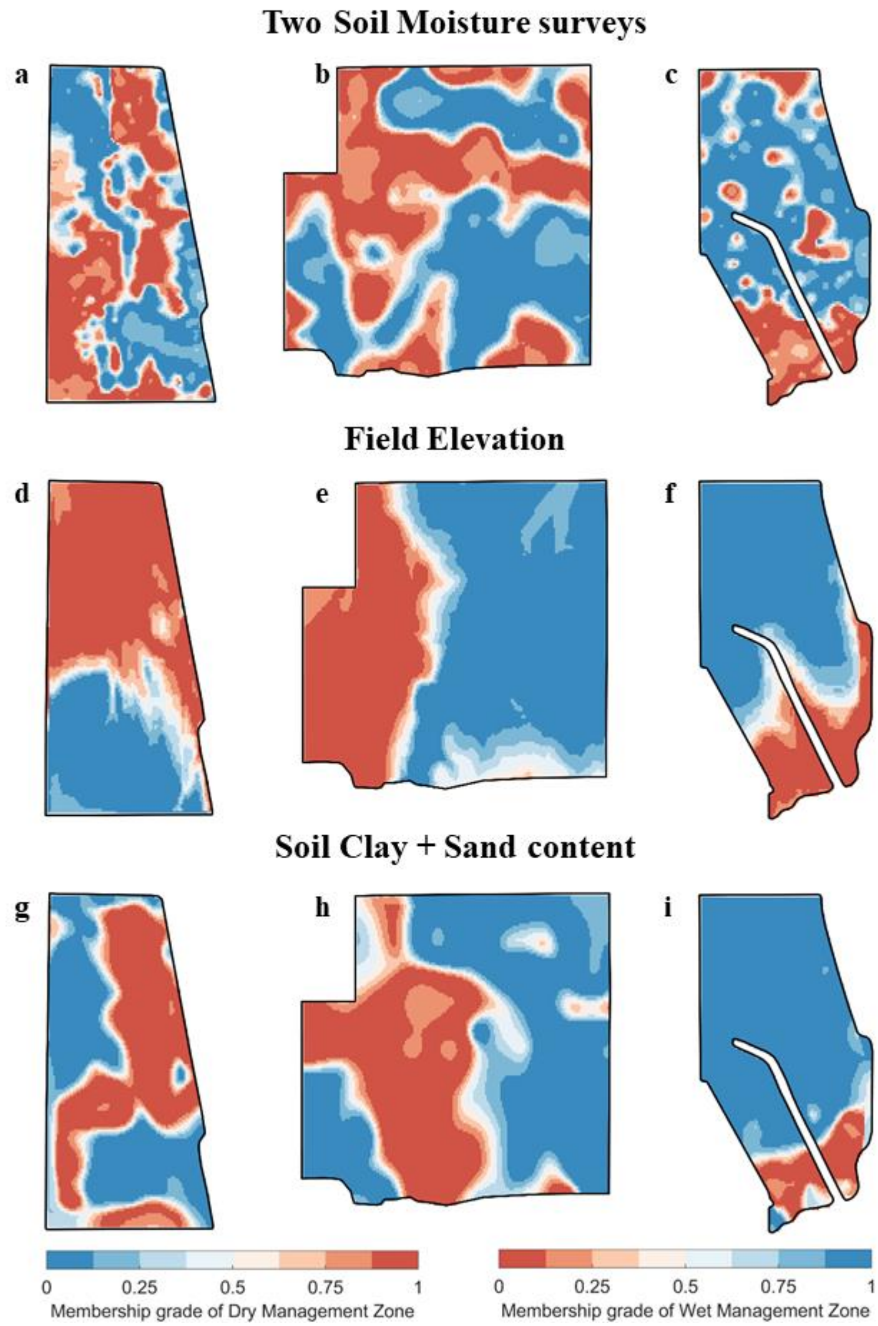

Figure 0.7**.** Alternative delineation of MZ using two soil moisture surveys (top), elevation (middle), and combined clay and sand fraction information (bottom) for Fields A (left), B (middle), and C (right).

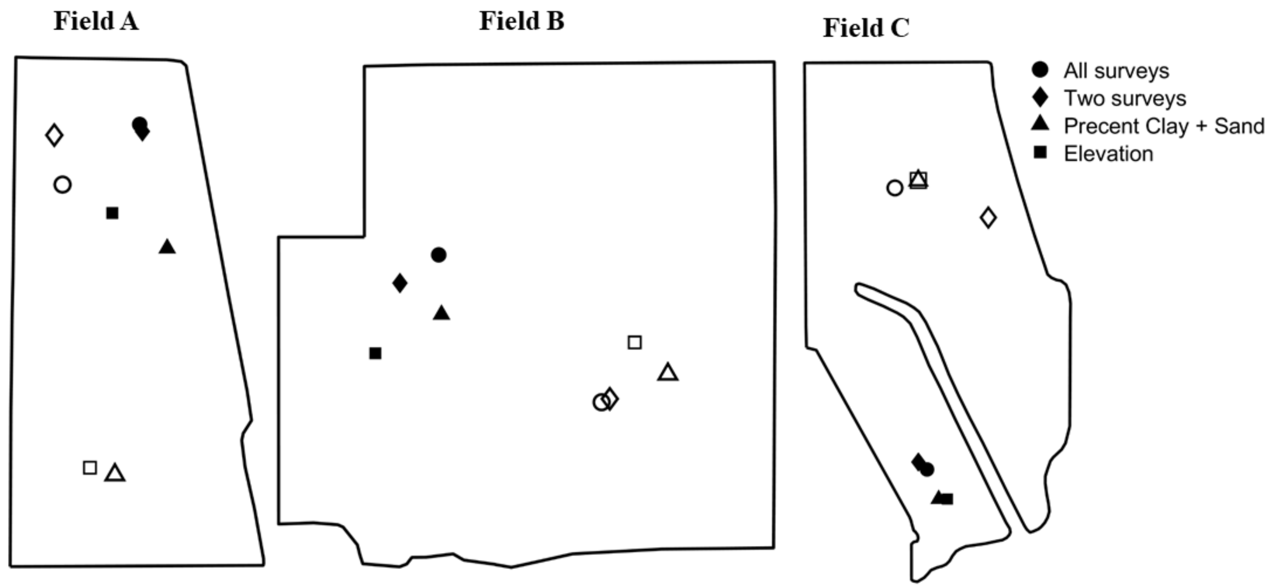

Figure 0.8**.** Sensitivity analysis for the tentative location of soil moisture sensors using soil all soil moisture surveys, only the driest and wettest soil moisture surveys, and proxy variables such as elevation and the fraction of clay and sand. Filled markers represent the sensor location in the dry MZ and hollow markers represent the sensor location in the wet MZ.

Chapter 3 - Predicting Rootzone Soil Moisture from Surface Observations in Agricultural Fields

Abstract

Rootzone soil moisture provides valuable information to guide in-season management decisions in rainfed and irrigated cropping systems. Measuring rootzone soil moisture usually requires the deployment of an array of multiple sensors along the soil profile, which can be labor intensive and costly. In this study we tested the skill of the exponential filter (EF) (Wagner et al., 1999) to infer rootzone soil moisture from a time series of in situ surface soil moisture observations in agricultural fields. Daily soil moisture observations from a sensor at 10 cm depth was used to predict the soil water content at 30 cm, 50 cm, 70 cm, and profile average in four sites under irrigated and rainfed conditions in central Kansas. The characteristic time length parameter was optimized for each site based on the Nash-Sutcliff (NS) score, the error between predicted and observed soil moisture was assessed using the NS score, the root means squared error (RMSE), and the mean bias error (MBE). The RMSE ranged from 0.133 to 0.206, and the MBE ranged from -0.57 to -0.01. Rootzone soil moisture predictions resulted most accurate when the entire soil profile was considered with average values across the four sites of RMSE of 0.049 $m^3\ m^{-3}$, correlation coefficient of 0.85, and MBE=-0.01 $m^3\ m^{-3}$. Site D achieved the most accurate soil moisture predictions with an average NS of 0.73, while Sites A showed the poorest performance with average NS scores of -0.08. The EF model resulted suitable for estimating rootzone soil moisture in only two out of four locations (NS> 0.5), particularly associated to sites with the shortest time series and a single crop during the study period. Our study shows that the phase of the crop rotation may have an added effect on the time characteristic parameter of the model separate from the effect of soil hydraulic properties, suggesting the need for a specific optimization of the time length parameter for each phase during the crop rotation.

Introduction

Rootzone soil water storage is one of the most important environmental factors limiting crop production in rainfed agricultural systems, particularly in semi-arid and sub-humid areas (Falkenmark et al., 2001), and a decisive variable dictating irrigation scheduling during the growing season (Hassanli et al., 2009; Irmak et al., 2012; Spencer, Falconer, et al., 2019). Accurate monitoring of rootzone soil moisture has resulted in increased crop water use efficiency improving the amount and timing of irrigation events, as well as crop yields and farm profits (Pereira, 2017). For instance, soil moisture-based irrigation scheduling in corn agricultural fields in Nebraska, U.S. resulted in 34% less irrigation application compared with farmer-managed fields (Irmak et al., 2012). Similarly, Spencer et al. (2019) working with data from irrigated fields in Arkansas found a 39% reduction in water use and an increase of corn grain yield by ~3% after analyzing multiple growing seasons. In United States, irrigated agriculture represents the second largest consumer of freshwater with 42% of the total withdraws in 2015 (Dieter et al., 2018), being responsible for nearly 50% of the total crop revenues (NASS, 2014).

A common method to estimate rootzone soil moisture in agricultural fields by researchers and consulting companies is to use semi-empirical and physically-based soil water balance models (Mishra et al., 2020). Semi-empirical models such as the dual crop coefficient method as described in the FAO-56 (Allen et al., 1998) has been widely used to simulate rootzone soil moisture for irrigation scheduling in corn, cotton, and orchards (Er-Raki et al., 2010; Payero et al., 2008; Thorp et al., 2017). More advanced physically-based soil water balance models such Hydrus (Šimůnek et al., 2008) have also been widely use to model rootzone soil moisture, particularly within applications of academic research. Crop models such as the Agricultural Production Systems Simulator (APSIM)(Keating et al., 2003) also offer an alternative to model rootzone soil moisture conditions by coupling a physically-based soil water balance model with advanced crop growth and development models. However, these models require information about field initial conditions, local forcing variables, depth-specific soil physical properties, and crop-specific parameters to accurately simulate the soil water balance during the growing season. While forcing variables such as precipitation and evapotranspiration can be obtained from local environmental monitoring networks, publicly available databases of soil physical properties have been mostly developed for natural resource planning and management applications at a coarser spatial scale relative to commercial agricultural fields (i.e. sub-kilometer level). As a consequence, accurate field-level estimations of rootzone soil moisture using these databases may result inaccurate at the field scale. In other words, the availability of site-specific soil physical properties is often the bottleneck for accurate predictions of rootzone soil moisture at the field scale using crop models.

Another alternative to quantify rootzone soil water storage in agricultural fields is to use point-level soil moisture sensors distributed along the soil profile. Soil moisture sensors are increasingly being adopted in irrigated cropping systems to provide timely and accurate soil moisture information for in-season irrigation scheduling and have been associated with important water savings ranging from marginal results up to 50% in single years, averaging ~20% in sub-humid areas, as well as maintaining crop yield and profitability (Evans et al., 2013; Kebede et al., 2014; Kukal et al., 2020; Sadler et al., 2005). Sensors based on electromagnetic principles are currently the predominant soil moisture sensing technology since these sensors can provide non-destructive and continuous estimates of soil moisture conditions along multiple growing seasons. These sensors offer relatively accurate (~0.03 m^3 m^{-3}) measurements over the full range of soil moisture conditions with minimum sensor maintenance (Adla et al., 2020; Dobriyal et al., 2012), and are typically integrated with data logging and telemetry systems for near-real time soil moisture monitoring. However, one important restriction of point-level sensors is the need for multiple sensors to characterize a given soil profile and the reduced support volume (<5 dm^3) compared to the volume of the rootzone across agricultural fields. Thus, multiple sensors need to be deployed in agricultural fields to accurately assess the rootzone soil moisture conditions, which becomes laborious, impractical, and costly to implement for local producers. Even though new commercially-available profile-level soil moisture sensors equipped with embedded sensors at multiple depths seem to have alleviated the installation problem, still the deployment of numerous soil moisture sensors to capture field-level rootzone soil moisture conditions can result costly. One possible solution to reduce the number and cost associated with deploying multiple soil moisture sensors to better cover the spatial extent of agricultural fields is to limit the monitoring of soil water content to shallow soil layers and then use a parsimonious model to predict soil moisture content over the soil profile. The portion of the soil profile near the soil surface typically exhibits the most dramatic changes in soil moisture due to wetting and drying events. This method would allow us to capture the rapidly and frequently changing soil moisture conditions in the topsoil layer with a sensor and then use a model to infer the soil moisture conditions at less variable soil depths.

Multiple semi-empirical models have been successfully used to depth-scale surface soil moisture observations such as the exponential filter (EF) (Wagner et al., 1999), maximum entropy model (Al-Hamdan and Cruise, 2010), and wavelets analysis (Grinsted et al., 2004). In particular, the EF has received particular interest from the remote sensing community to estimate profile-level soil moisture conditions from shallow (0-5 cm) measurements of soil water content from dedicated satellite missions such as the Soil Moisture Active-Passive and the Soil Moisture and Ocean Salinity missions (Entekhabi et al., 2010). The EF is attractive because of the minimal number of required parameters and the possibility to account for intermittently available surface soil moisture observations (Albergel et al., 2008; Mishra et al., 2020). For example, Ceballos et al. (2005) using the EF found a strong significant correlation (R^2= 0.75) between rootzone (0 to 100 cm) soil moisture derived from European Remote Sensing Satellite (ERS) scatterometer retrievals and in situ soil moisture observations in the Duero Basin in Spain. In a study using in situ surface soil moisture observations to predict rootzone (i.e. 0-50 cm) soil moisture under grassland vegetation across two sparse networks in United States, Wang et al. (2017) found an correlation coefficient between a normalized soil water index between soil layers of R^2= 0.65 with, RMSE=0.22, and MBE=0.03. Similarly, Peterson et al. (2016) working on a 25-hectare grazing pasture in Canada concluded that the EF has the greatest potential to estimate rootzone soil moisture derived from near-surface soil moisture estimated from cosmic-ray neutron observations when compared to time–stable monitoring locations and representative landscape units.

Although substantial research has been reported using EF to retrieve rootzone soil moisture from remote sensing products over large areas (i.e. ten of kilometers) and from in situ soil moisture observations in landscapes dominated by natural grassland vegetation, there is a gap about employing the EF method to estimate rootzone soil moisture from near-surface in situ soil observations in agricultural fields. We hypothesize that a single shallow soil moisture sensor coupled with the exponential filter will result in rootzone soil moisture estimates that are comparable to a dense array of sensors across the soil profile. The objective of this study was to investigate the accuracy of an exponential filter coupled with daily in situ observations of surface soil moisture to estimate daily rootzone soil water storage. The proposed method has the potential to reduce the number of sensors required per monitoring location, allowing producers, researchers, and water managers to increase the number of monitoring locations to better characterize rootzone soil moisture across the field.

Materials and methods

Sites and datasets

Field-level soil moisture observations were collected in three different agricultural fields in central Kansas from October 2016 to September 2020 (Table 1). Site A, is situated within the Kansas State University North Agronomy Farm Experiment Research Station near Manhattan, KS. The cropping system of Site A follows a no-till rotation based on winter wheat, double crop soybean, and full season sorghum under rainfed conditions. Site B is situated near Hutchinson, KS and the cropping system consists of a minimum tillage operation with a full season corn and soybeans rotation under a center pivot irrigation. Sites C and D were both situated in an irrigated field with no-till crop rotation near Moundridge, KS, but each site was located in zones of the field with distinct soil type and topographic conditions. Site C was located at the bottom slope characterized by the Farnum series with loam soils (slopes 1 to 3%) with the presence of fine gravel in the top soil horizons (Soil Survey Staff, 2020). Site D was located on upland area characterized by deep and moderately well drained Crete series with silt loam soils with <1% slopes (Soil Survey Staff, 2020). Sites C and D were intentionally located in the same field following the results of a previous research study in the same field that subdivided the field into two distinct soil moisture-based management zones. The length of surface soil moisture time series collected varied among experimental Sites according to the availability of each field for research purposes. Time series ranged from 66 days (Site B) to 572 days (Site C) resulting in diverse number of monitored crops on each Site (Table 1). The region encompassing the three fields has an average annual rainfall of 800 mm, a mean annual temperature of 13 ºC, and a mean minimum and maximum air temperature between -1 ºC and 27 ºC.

At each site we deployed an in situ soil moisture monitoring station consisting of datalogger (CR200X, Campbell Scientific, Logan, UT, USA) equipped with four soil water reflectometers (CS655, Campbell Scientific). The soil moisture sensors consist of two 12-cm long stainless steel rods attached to an epoxy sensor head. All output variables from the sensor are sampled every 15 seconds and are averaged hourly, and daily intervals. All raw variables reported by the sensor are saved including voltage ratio, relative permittivity, temperature, period average, and electrical conductivity. Electronic components were placed into an all-weather enclosure and the station was powered by a 10 W solar panel. For this study we assumed an 80-cm soil profile that was divided into 4 layers of 20 cm each. Sensors were installed by first creating a trench and then inserting each sensor horizontally into the undisturbed face of the trench at 10, 30, 50, and 70 cm depth (Figure 1). Each sensor depth is assumed to be located at the center of the layer that it represents. For instance, the sensor deployed at 10 cm depth represents the soil water content of the 0-20 cm soil layer. The daily profile soil water storage was computed as follows:

$$S_t = \sum_{i=1}^{4}(\theta_{it} z) \quad [2]$$

where S_t is the storage soil moisture (mm) on day *t*, the $\theta_{i,t}$ is the volumetric water content of layer *i* on day *t*, and *z* is the depth of the soil layer (mm).

All sensor output variables, including soil temperature, dielectric permittivity, bulk electrical conductivity, and period average were recorded at hourly intervals. A custom sensor calibration equation was developed under laboratory conditions using columns with packed soil from different parts of the fields and known volumetric water content from the packed columns were used to fit a linear regression model as a function of a linear model of the squared root of the dielectric permittivity measured by the sensor (Ledieu et al., 1986):

$$\theta = -0.0994 + 0.0968\sqrt{Ka} \quad [1]$$

where θ (m^3 m^{-3}) is the volumetric water content and K_a(unitless) is the real part of the dielectric permittivity, and the two empirical parameters were obtained by optimization of the model based on ordinary least squares by using *lsqcurvefit* function in Matlab 2018 b (Mathworks, Natick, MA). During the winter time, and few times during the growing season, malfunctioning batteries and solar panels introduced some gaps in the temporal record. As a result, we only used soil moisture data for growing seasons and fallow periods with no missing observations. Soil moisture observations when the soil temperature was <4 °C were removed due to changes in the dielectric permittivity of soil water (Seyfried and Grant, 2007) and replaced with a moving median filter with a 60 days window.

Exponential filter method

The exponential filter is a semi-empirical approach proposed by Wagner et al. (1999) and later reformulated in a recursive form by Albergel et al. (2008) with the aim of estimating rootzone soil moisture from surface soil moisture observations. This method simplifies the soil water balance using a two-layer approach, where the flux between these two layers is proportional to the difference in soil moisture content between the layers. The model assumes a constant pseudo-diffusivity factor that propagates fluctuations in surface soil moisture in attenuated form to deeper soil layers. The recursive formulation to retrieve rootzone soil moisture from surface soil moisture observations can be expressed as:

$$SWI_{m(n)} = SWI_{m(n-1)} + K_n(ms_{(n)} - SWI_{m(n-1)}) \quad [3]$$

where SWI_m is the soil water index at the rootzone, ms_n is the normalized soil moisture observed at the surface layer, n represent the time in days, and K is the gain function (range from 0 to 1) that is computed as:

$$K_n = \frac{K_{n-1}}{K_{n-1} + e^{\frac{t_n - t_{n-1}}{T}}} \quad [4]$$

where $t_n - t_{n-1}$ is the difference in days between surface soil moisture observations (a value of 1 in our study), and T is an empirical characteristic time length in days and the only unknown of the model. The parameter T is often assumed to represent soil hydraulic properties and the vertical anisotropy of the soil profile characterized by different soil texture and bulk density of the soil horizons that affect the temporal dynamics of soil moisture within the soil profile (Albergel et al., 2008; Ceballos et al., 2005). Therefore, the T parameter should be calibrated on each individual study site. To optimize the value of T parameter (T_{op}), SWI_m was computed using different values of T (1 to 60 days) (Wang et al., 2017). The Nash-Sutcliffe (NS) score (Nash and Sutcliffe, 1970) was used to evaluate the performance of the EF (Albergel et al., 2008; Ford et al., 2014; Wang et al., 2017). The NS score can range from $-\infty$ to 1, where a value of 1 corresponds to a perfect match between predicted and observed data, while values lower than 0 typically represent that the observed mean is a better predictor than the approximation made using the exponential filter. In addition, to evaluate the EF performance correlation coefficient (r), root mean squared error (RMSE), and mean bias error (MBE) were computed.

To obtain ms_n, observed volumetric water content at 10 cm depth was normalized with a mean of 0 and a standard deviation of 1 (i.e. *zscore*). Daily observations of rootzone also was normalized to obtain the observed soil water index $SWI_{(Obs)}$. For initialization of the EF we assumed that $SWI_{m(1)} = ms_{(1)}$ and $K_1 = 1$ (Albergel et al., 2008).

Results and discussion

The exponential filter was used to estimate rootzone soil water storage from available surface soil moisture observations at four different sites from October 2016 to March 2020 (Table 1). Normalized daily volumetric soil water content ms_n at 10 cm depth was used to predict SWI_m at 30 cm, 50 cm, and 70 cm, as well as the profile average from 0 to 80 cm depth.

Base on the Nash-Sutcliffe score, Site D achieved the most accurate soil moisture predictions with an average NS of 0.73, while Sites A and C showed the worst performance with average NS scores of -0.08 and 0.09, respectively (Table 2). Sites A and C both spanned two crops during the study period with significant changes on vegetation coverage and crop root water uptake, with negative NS scores values at 50 and 70 cm reaching values below -0.5 (Table 2). On the contrary, Sites B and D spanned periods with a single crop and had higher average NS scores ranging from 0.55 and 0.73, respectively. Our results suggest that the exponential model may fail to capture changes in the rootzone soil moisture related to changes in the land cover. This deficiency could be attributed to the fact that surface soil moisture dynamics in the 0-20 cm depth and the rootzone soil moisture dynamics in the 20-80 cm depth followed different patterns along the different land covers, which can directly affect the performance of the EF (Albergel et al., 2008; Ford et al., 2014; Wang et al., 2017). Our results also suggest that for better model performance either the T parameter would need to be fitted to each specific land cover or an additional empirical factor needs to be added to the model to account for the different patterns of root water uptake and sub-soil soil moisture dynamics. Previous studies using the EF in in-situ soil moisture information have primarily involved observations under natural grassland conditions from sparse networks, which likely do not exhibit the contrasting changes in surface and sub-surface soil moisture dynamics of agricultural fields. Under natural grassland conditions, it is possible that a single calibrated T parameter is able to capture the soil hydraulic properties and the seasonal changes in vegetation, while in agricultural fields conditions the different phases of the crop rotation may lead to an average T parameter that cannot capture well the conditions of winter and summer crops and the presence of fallow periods.

Across all depths and sites, the RMSE values of the soil water index ranged from 0.105 to 0.301 with mean of 0.173. Given the average soil moisture content and the average RMSE at each depth, an estimate of the average error soil moisture retrieval is about 0.063 $m^3 m^{-3}$ at 30 cm, 0.079 $m^3 m^{-3}$ at 50 cm, 0.067 $m^3 m^{-3}$ at 70 cm, and 0.049 $m^3 m^{-3}$ for the profile average. Our findings stand above those reported values retrieved from in situ soil moisture networks on grasslands fields in United States (Wang et al., 2017) and in France (Albergel et al., 2008). In general, the Pearson correlation coefficient showed high degree of concordance between surface observation and the deeper layers (r= 0.77). Typically, r values >0.7 are associated with positive NS values, however, there were occasions (e.g. Site A at 70 cm, Table 2) in which the EF resulted in a relatively high correlation (r= 0.79) but the NS score was remarkably low (NS=-0.67). This discrepancy may be caused by a strong bias and decoupled conditions between surface and sub-surface soil layers due to the presence of an actively growing vegetation and vertical changes in soil texture (Calvet and Noilhan, 2000).

Parameter T, was optimized for each site based on the highest NS score (Table 2). Average values of T_{op} ranged from 1 day in Site B to 17 days in Site A, with a clear variation across sites and depths matching previous findings by (Albergel et al., 2008). Sharp changes in T_{op} were observed in Site A and Site C at 50 cm depths coinciding with the highest values of MBE=-1.85 and MBE=0.23, respectively. Sharp transitions due to the presence of soil horizons with different soil hydraulic properties are not accounted by the EF model, and deviations from the assumption of homogeneity can negatively affect the performance of the model. Despite the limited number of fields in this study, our findings are in agreement with previous woks by Wang et al. (2017), in which T_{op} showed a negative correlation with sand content (R2=0.66).

Rootzone SWI prediction

The soil water index was predicted at rootzone depths of 30, 50, and 70 cm on each site (Figure 2). Predictions of the soil water index were most accurate at depths of 30 cm with mean NS of 0.49, while predictions of soil water index using the EF at 50 cm had the poorest performance with mean NS of 0.21 (Table 2). Not surprisingly, the similar soil moisture dynamics between the 0-20 cm layer and the 20-40 cm layer resulted in good coupling strength, and hence the accurate predictions throughout multiple sites (Ceballos et al., 2005; Wang et al., 2017; Yari et al., 2017). On the other hand, soils with clear horizon stratifications usually showed important contrast on soil texture between the surface layer and deep layers (i.e. 50 cm), restraining the vertical soil moisture redistribution and disrupting the coupling strength across the soil column. Further analysis on each site, showed that either Site A and Site C both with poor EF performance presented negative NS score at 50 cm depth (Table 2), where estimated and observed SWI clearly show a discrepancy across the study period (Figure 2). Wang et al. (2017) estimating SWI at 50 cm depth on under grasslands conditions across the Soil Climate Analysis Network (SCAN) also found negative mean NS values (NS= -0.50). This limitation at 50 cm could be attributed to active root water uptake coupled with temporal delays for soil moisture redistribution between the soil surface and the deeper layers of the soil profile (Weaver and Darland, 1949).

A clear example of contrasting SWI dynamics between soil layers at 30, 50, and 70 cm depth was observed in Site C from May to September 2020 (Figure 2). The SWI presented high variability associated with crop water uptake and frequent irrigation events. The EF model was able to accurately predict SWI at 30 cm, but was unable to capture the dynamics at 50 and 70 cm depths. Further inspection of the soil profile revealed that the weak coupling strength between soil layers were likely caused by drastic changes in the soil texture thought the soil column. From personal experience while installing the sensors observed soil texture changed from fine sandy loam with the presence of fine gravel at surface layer to a clay loam layer between 30 to 50 cm and finally a sandy clay loam texture with fine gravel from 50 to 80 cm. Different patterns in soil texture and soil moisture content can also influence the root distribution and root activity of the crop, further contributing to decoupled dynamics between surface conditions and rootzone conditions. Our results agree well with those of Ford et al. (2014), who conclude that the EF can provide accurate estimations of rootzone soil moisture as long as the soil characteristics are relative homogeneous through the soil column.

Profile average SWI from 0 to 80 cm depth was predicted using the EF resulting in the best SWI predictions compared with the previous analyzed soil depths at 30, 50, and 70 cm. Considering all sites profile SWI prediction showed the highest mean NS score with a value of 0.56, the highest mean Pearson correlation coefficient r= 0.85, and smallest mean RMSE=0.13 (~

40 mm of water) (Table 2). During the growing season, the predicted profile SWI exhibited clear and sometimes sharp declines in profile soil water index as a result of the water uptake by the actively growing vegetation (Corn crop in Site C, Figure 3), while during the fallow periods the profile was slowly recharged and showed relatively smoother fluctuations in soil water storage (Fallow period in Site C, Figure 3). Exploring the model error dynamics across the different phases of the crop rotation revealed that low errors between predicted and observed SWI were mainly associated with fallow periods containing ~60 to 70% of soil coverage by crop residues at the soil surface promoting the soil water recharge (e.g. Sites C and D). Soil moisture recharge periods increase the coupling strength between surface observations and deeper layer (Mahmood et al., 2012), increasing the prediction accuracy of the EF (Ford et al., 2014). On the other hand, during periods of active crop growth, especially when both soil evaporation and crop water uptake are at a maximum rate (e.g. corn near anthesis), predicted profile SWI showed maximum errors (e.g. Figure 3 Site C, during corn seasons 2019 and 2020). The EF model showed low accuracy on fields with heterogeneous soil profiles minimum requirement of model predictions (NS> 0.3).

Considering the average RMSE of 40 mm of water within the soil profile our methodology not seems to be appropriate to guide scheduling irrigations. Previous research works estimating soil water storage to guide irrigation strategies in center pivot irrigated corn in northeast Colorado have reported values of 16 mm (0 to 105 cm profile) an error that can be compensated by a single irrigation event (Andales et al., 2015).

Conclusion

The proposed method of estimating rootzone soil moisture by only deploying a surface sensor couple with an exponential filter presents clear practical advantages over excavating and deploying multiple sensors along the soil profile of large agricultural fields. Across four sites of varied soil texture and management practices, the characteristic time length parameter was optimized T_{op} showing variability between sites, depths, and a negative correlation with sand content. Predictions using the exponential filter resulted most accurate when considering the full soil profile, followed by predictions on the sub-soil layer immediately below the sensor layer (i.e. 20-40 cm layer with sensor at 30 cm). The timing and spatial patterns in crop water uptake along the rootzone likely caused a disparity between surface and sub-surface soil water dynamics that was not captured by the model using a single time characteristic length parameter. The models resulted suitable for estimating rootzone soil moisture in only two out of four locations, particularly in fields with a single crop during the study period. The proposed method does not seem adequate to advise irrigation scheduling considering an average RMSE with a value of 0.049 $m^3 m^{-3}$ for the entire soil profile, which would translate into an error of about 40 mm or approximately 30% of the total available water storage of the profiles.

There still remains a considerable gap in the research literature about the application of the exponential filter in agricultural fields conditions along multiple phases of the crop rotation. Future studies using the exponential filter in agricultural fields conditions should focus on determining the separate effect of soil hydraulic properties and crop sequence, and should explore the possibility to implement a changing T parameters that can account for the different phases of the crop rotation. The proposed method has the potential to either reduce costs associated with sensor hardware or to increase the area of the field covered with a given number of sensors relative to the alternative of deploying most of these sensors at greater soil depths. This approach could become particularly useful as new wireless sensors for surface soil moisture monitoring become commercially available. The proposed method could transform a swarm of spatially distributed near-surface soil moisture sensors into field-level rootzone soil moisture to better guide irrigation scheduling.

References

Adla, S., Rai, N. K., Karumanchi, S. H., Tripathi, S., Disse, M., & Pande, S. (2020). Laboratory Calibration and Performance Evaluation of Low-Cost Capacitive and Very Low-Cost Resistive Soil Moisture Sensors. Sensors, 20(2), 363. https://doi.org/10.3390/s20020363

Al-Hamdan, O. Z., & Cruise, J. F. (2010). Soil Moisture Profile Development from Surface Observations by Principle of Maximum Entropy. Journal of Hydrologic Engineering, 15(5), 327–337. https://doi.org/10.1061/(asce)he.1943-5584.0000196

Albergel, C., ¨ Udiger, C. R., Pellarin, T., Calvet, J.-C., Fritz, N., Froissard, F., Suquia, D., Petitpa, A., Piguet, B., & Martin, E. (2008). Hydrology and Earth System Sciences From near-surface to root-zone soil moisture using an exponential filter: an assessment of the method based on in-situ observations and model simulations. In Hydrol. Earth Syst. Sci (Vol. 12). www.hydrol-earth-syst-sci.net/12/1323/2008/

Allen, R. G., Pereira, L. S., Raes, D., & Smith, M. (1998). Crop evapotranspiration-Guidelines for computing crop water requirements. Guidelines for Computing Crop Water Requirements-FAO Irrigation and Drainage Paper 56. FAO Rome, 300(9), 109.

Calvet, J. C., & Noilhan, J. (2000). From near-surface to root-zone soil moisture using year-round data. Journal of Hydrometeorology, 1(5), 393–411. https://doi.org/10.1175/1525-7541(2000)001<0393:FNSTRZ>2.0.CO;2

Ceballos, A., Scipal, K., Wagner, W., & Martínez-Fernández, J. (2005). Validation of ERS scatterometer-derived soil moisture data in the central part of the Duero Basin, Spain. Hydrological Processes, 19(8), 1549–1566. https://doi.org/10.1002/hyp.5585

Dobriyal, P., Qureshi, A., Badola, R., & Hussain, S. A. (2012). A review of the methods available for estimating soil moisture and its implications for water resource management. In Journal of Hydrology (Vols. 458–459, pp. 110–117). Elsevier. https://doi.org/10.1016/j.jhydrol.2012.06.021

Evans, R. G., LaRue, J., Stone, K. C., & King, B. A. (2013). Adoption of site-specific variable rate sprinkler irrigation systems. In Irrigation Science (Vol. 31, Issue 4, pp. 871–887). https://doi.org/10.1007/s00271-012-0365-x

Falkenmark, M., Fox, P., Persson, G., & Rockström, J. (2001). Water Harvesting for Upgrading of Rainfed Agriculture: Problem Analysis and Research Needs, SIWI Report II.

Ford, T. W., Harris, E., & Quiring, S. M. (2014). Estimating root zone soil moisture using near-surface observations from SMOS. Hydrology and Earth System Sciences, 18(1), 139–154. https://doi.org/10.5194/hess-18-139-2014

Grinsted, A., Moore, J. C., & Jevrejeva, S. (2004). Nonlinear Processes in Geophysics Application of the cross wavelet transform and wavelet coherence to geophysical time series (Vol. 11). http://www.pol.ac.uk/home/research/waveletcoherence/

Irmak, S., Burgert, M. J., Yang, H. S., Cassman, K. G., Walters, D. T., Rathje, W. R., Payero, J. O., Grassini, P., Kuzila, M. S., Brunkhorst, K. J., Eisenhauer, D. E., Kranz, W. L., Vandewalle, B., Rees, J. M., Zoubek, G. L., Shapiro, C. A., & Teichmeier, G. J. (2012). Large-scale on-farm implementation of soil moisture-based irrigation management strategies for increasing maize water productivity. 55(3), 881–894.

Keating, B. A., Carberry, P. S., Hammer, G. L., Probert, M. E., Robertson, M. J., Holzworth, D., Huth, N. I., Hargreaves, J. N., Meinke, H., Hochman, Z., & McLean, G. (2003). An overview of APSIM, a model designed for farming systems simulation. European Journal of Agronomy, 18(3–4), 267–288.

Kebede, H., Fisher, D. K., Sui, R., & Reddy, K. N. (2014). Irrigation Methods and Scheduling in the Delta Region of Mississippi: Current Status and Strategies to Improve Irrigation Efficiency. American Journal of Plant Sciences, 05(20), 2917–2928. https://doi.org/10.4236/ajps.2014.520307

Kukal, M. S., Irmak, S., & Sharma, K. (2020). Development and application of a performance and operational feasibility guide to facilitate adoption of soil moisture sensors. Sustainability (Switzerland), 12(1). https://doi.org/10.3390/su12010321

Ledieu, J., De Ridder, P., De Clerck, P., & Dautrebande, S. (1986). A method of measuring soil moisture by time-domain reflectometry. Journal of Hydrology, 88(3–4), 319–328. https://doi.org/10.1016/0022-1694(86)90097-1

Mahmood, R., Littell, A., Hubbard, K. G., & You, J. (2012). Observed data-based assessment of relationships among soil moisture at various depths, precipitation, and temperature. Applied Geography, 34, 255–264. https://doi.org/10.1016/j.apgeog.2011.11.009

Mishra, V., Lee Ellenburg, W., Markert, K. N., Limaye, A. S., & Pingale, S. (2020). Performance evaluation of soil moisture profile estimation through entropy-based and exponential filter models Performance evaluation of soil moisture profile estimation through entropy-based and exponential filter models Performance evaluation of soil mo. Hydrological Sciences Journal, 65(6), 1036–1048. https://doi.org/10.1080/02626667.2020.1730846

Nash, J. E., & Sutcliffe, J. V. (1970). River flow forecasting through conceptual models part I - A discussion of principles. Journal of Hydrology, 10(3), 282–290. https://doi.org/10.1016/0022-1694(70)90255-6

NASS, U. (2014). Farm and Ranch Irrigation Survey (2013). Farm and Ranch Irrigation Survey (2013); National Agricultural Statistics Service, Ed.; United States Department of Agriculture:, 3, 266.

Pereira, L. S. (2017). Water, Agriculture and Food: Challenges and Issues. Water Resources Management, 31(10), 2985–2999. https://doi.org/10.1007/s11269-017-1664-z

Peterson, A. M., Helgason, W. D., & Ireson, A. M. (2016). Estimating field-scale root zone soil moisture using the cosmic-ray neutron probe. Hydrology and Earth System Sciences, 20(4), 1373–1385. https://doi.org/10.5194/hess-20-1373-2016

Sadler, E. J., Evans, R. G., Stone, K. C., & Camp, C. R. (2005). Opportunities for conservation with precision irrigation. Soil Water Conservation, 60, 371–379. https://pubag.nal.usda.gov/download/18977/PDF

Seyfried, M. S., & Grant, L. E. (2007). Temperature Effects on Soil Dielectric Properties Measured at 50 MHz. Vadose Zone Journal, 6(4), 759–765. https://doi.org/10.2136/vzj2006.0188

Soil Survey Staff. (2020). Soil Survey Staff, Natural Resources Conservation Service, United States Department of Agriculture. https://websoilsurvey.sc.egov.usda.gov/. Accessed 26 January 2021

Spencer, G. D., Krutz, L. J., Falconer, L. L., Henry, W. B., Henry, C. G., Larson, E. J., Pringle III, H. C., Bryant, C. J., & Atwill, R. L. (2019). Irrigation Water Management Technologies for Furrow-Irrigated Corn that Decrease Water Use and Improve Yield and On-Farm Profitability. Crop Forage Turfgrass Manage.

Wagner, W., Lemoine, G., & Rott, H. (1999). A method for estimating soil moisture from ERS Scatterometer and soil data. Remote Sensing of Environment, 70(2), 191–207. https://doi.org/10.1016/S0034-4257(99)00036-X

Wang, T., Franz, T. E., You, J., Shulski, M. D., & Ray, C. (2017). Evaluating controls of soil properties and climatic conditions on the use of an exponential filter for converting near surface to root zone soil moisture contents. Journal of Hydrology, 548, 683–696. https://doi.org/10.1016/j.jhydrol.2017.03.055

Weaver, J. E., & Darland, R. W. (1949). Soil-root relationships of certain native grasses in various soil types. Wiley on Behalf of the Ecological Society of America - Ecological Monographs, 19(4), 303–338.

Yari, A., Madramootoo, C. A., Woods, S. A., Adamchuk, V. I., & Huang, H.-H. (2017). Assessment of Field Spatial and Temporal Variabilities to Delineate Site-Specific Management Zones for Variable-Rate Irrigation. Journal of Irrigation and Drainage Engineering, 143(9), 04017037. https://doi.org/10.1061/(ASCE)IR.1943-4774.0001222

Table 0.1. Site, crop rotation, study period, and top 15 cm soil textural class, percentage of clay, sand, and silt fractions.

Site	Crop rotation†	Start date	End date	Total days	Number of Crops¶	Soil Textural class‡	Soil series
A	WW-SB	25-Oct-16	29-Oct-17	369	2	Silt loam	Kahola
B	CN	22-Jun-18	27-Aug-18	66	1	Sandy loam	Avans
C	CN-FW	26-Apr-19	18-Nov-20	572	2	Loam	Farnum
D	CN-FW	24-Apr-19	31-Mar-20	342	1	Silty clay loam	Crete

† WW=Winter wheat; SB=Soybean; FW=Fallow; CN=Corn
‡ Soil textural class based on the sand and clay content in the top 0-15 cm. Site A texture data was obtained from Soil Survey Geodatabase (SSURGO, (Soil Survey Staff, 2020). Site B, C, D information was obtained from disturbed (0-15cm) soil samples characterized using the hydrometer method (Gavlak et al., 2003)
¶ Number of crops occurred during the study period.

Table 0.2. Characteristic time length parameter optimization ($\boldsymbol{T_{op}}$) for each site-depth, and Nash-Sutcliffe (NS), root mean square error (RMSE), Pearson correlation coefficient (*r*), and mean bias error (MBE) statistic scores for the correlation between the $\boldsymbol{SWI_{obs}}$ and $\boldsymbol{SWI_m}$. Normalized surface soil moisture at 10 cm was used to predict $\boldsymbol{SWI_m}$ and $\boldsymbol{T_{op}}$ at 30 cm, 50 cm, 70 cm, and profile average.

Site	Depth	T_{op}	NS	RMSE	r	MBE
A	cm	days				
	30	12	0.39	0.136	0.59	-0.08
	50	28	-0.31	0.256	0.64	-1.85
	70	19	-0.67	0.264	0.79	-0.23
	Profile mean	10	0.27	0.144	0.84	-0.11
B	30	1	0.62	0.150	0.79	-0.01
	50	1	0.57	0.161	0.76	0.01
	70	1	0.31	0.173	0.89	0.14
	Profile mean	1	0.70	0.138	0.85	0.02
C	30	3	0.09	0.212	0.72	0.15
	50	10	-0.50	0.301	0.64	0.23
	70	7	0.33	0.166	0.59	-0.01
	Profile mean	2	0.44	0.145	0.79	0.08
D	30	6	0.65	0.171	0.82	0.03
	50	5	0.67	0.129	0.83	-0.02
	70	8	0.75	0.128	0.88	-0.03
	Profile mean	2	0.83	0.105	0.92	-0.03

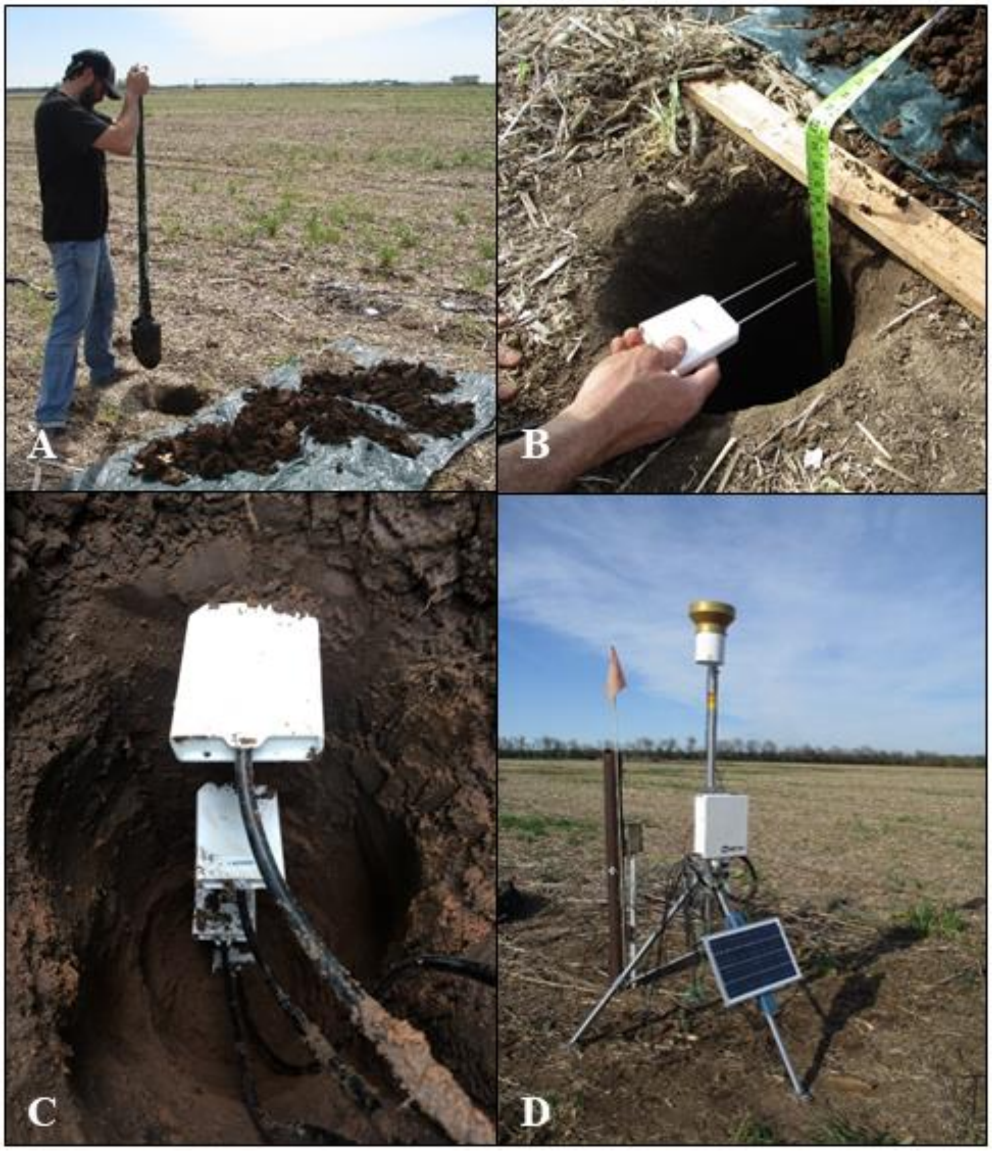

Figure 0.1. A) Excavation of a small trench while maintaining soil layers separately; B) installation of soil water reflectometers at specific depths from the soil surface; C) set of four soil moisture sensors installed horizontally into the undisturbed face of the trench at 10, 30, 50, and 70 cm depth on Site B; and D) side-view of the monitoring station in Site D showing a tipping-bucket rain gauge, a solar panel, and an all-weather enclosure mounted on a tripod. The trench was about 10 meters from the tripod.

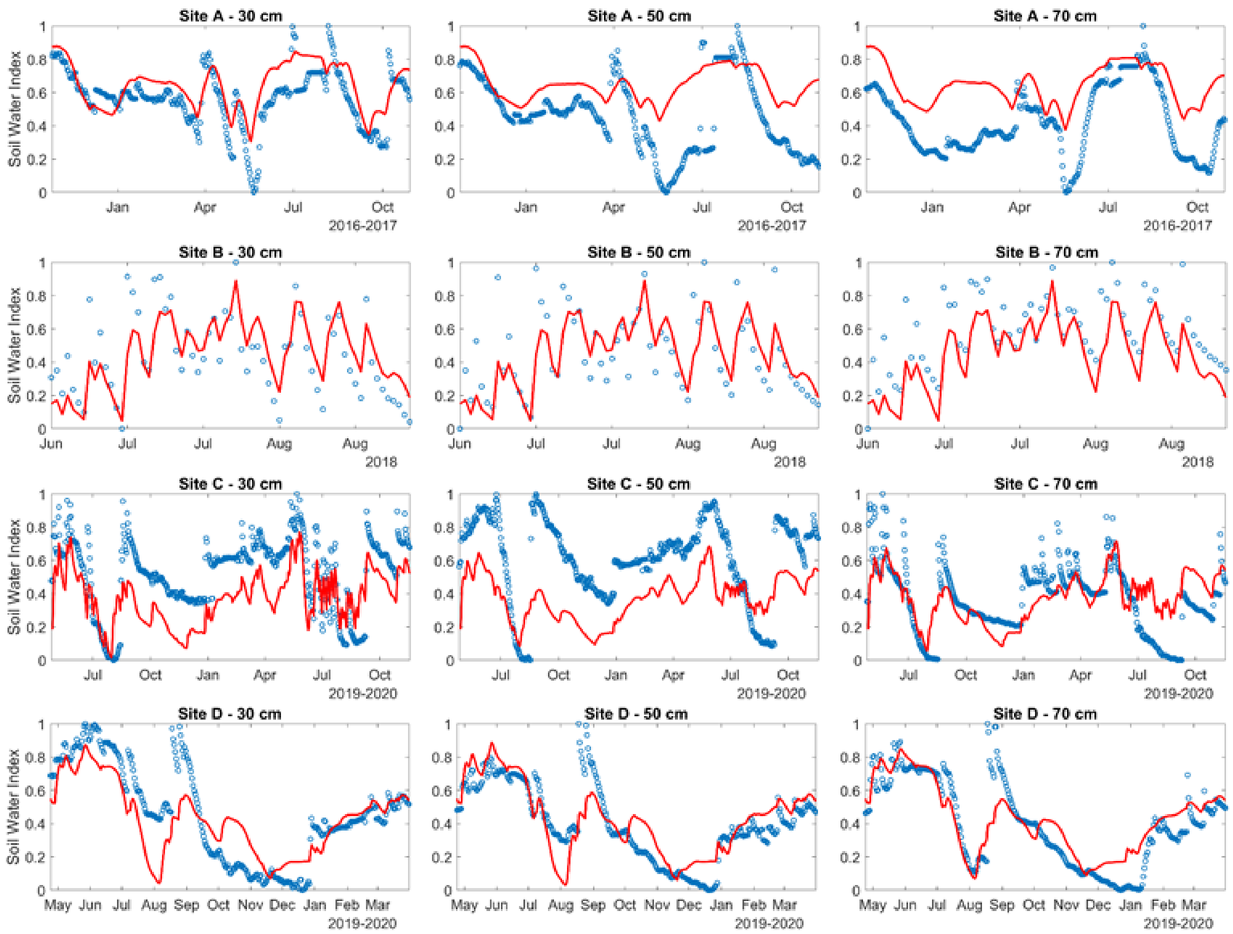

Figure 0.2. Predicted ($\boldsymbol{SWI_m}$, red line) and observed soil water index ($\boldsymbol{SWI_{obs}}$, blue markers) at 30 cm, 50 cm, and 70 cm soil depths for each site.

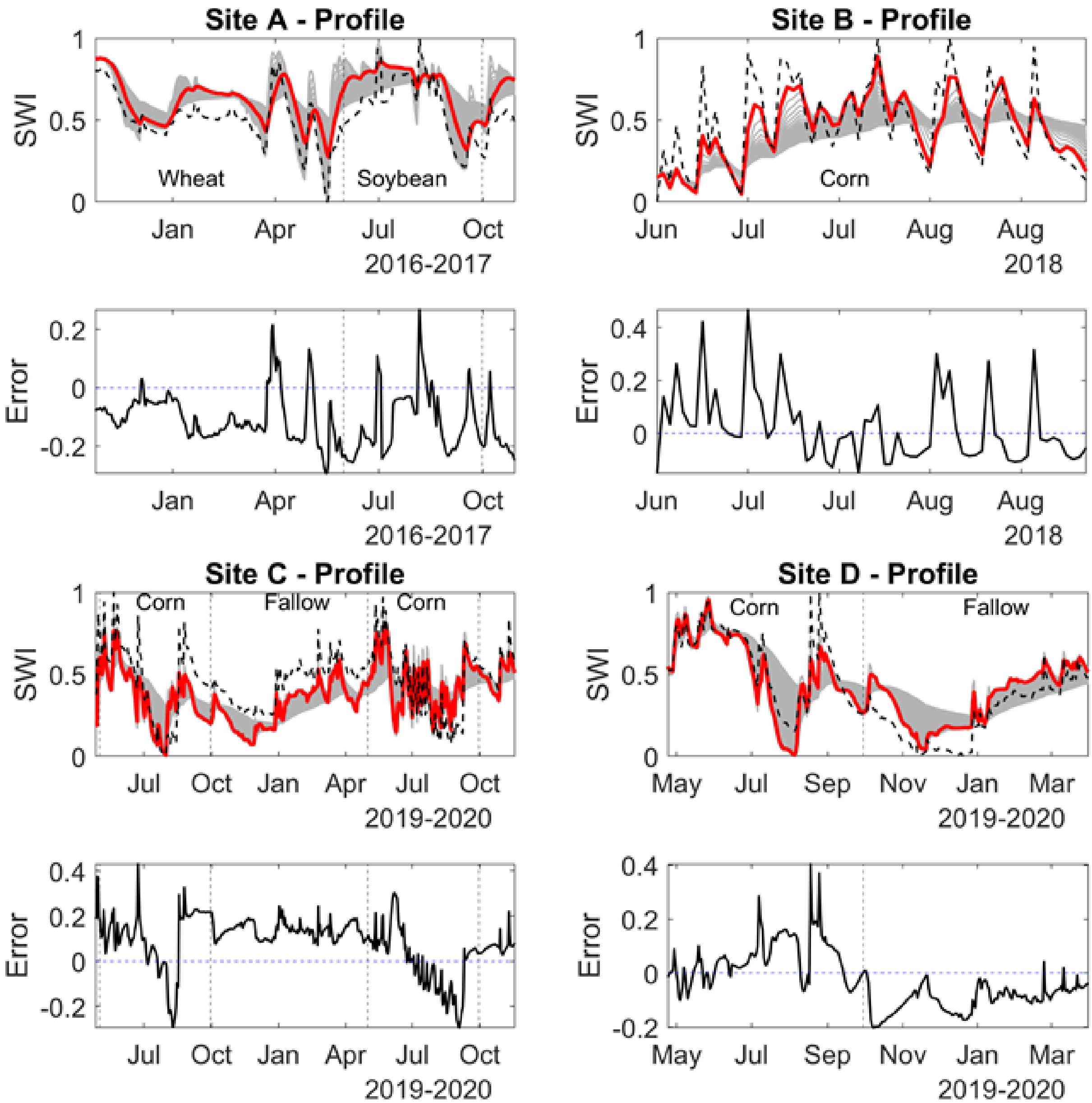

Figure 0.3. Predicted ($\boldsymbol{SWI_m}$, red solid line) and observed ($\boldsymbol{SWI_{obs}}$, black dash line) mean profile (0-80 cm) soil water index prediction for each site. Grey solid lines represent multiple simulations of predicted soil water index by ranging the value of the parameter $\boldsymbol{T}$ optimization. For each site, the error (observed - predicted) is presented on a separate subplot (black solid line) below each SWI plot. Vertical dashed lines depict the limits between the phases of the crop rotation.

Chapter 4 - General Conclusions

Water is a critical input for agricultural production and represents the second major consumer of freshwater withdraws in United States. In the state of Kansas, about 1 million hectares are cultivated every year under irrigated conditions in regions that currently face some degree of water shortages as a result of declining groundwater resources. Thus, accurate monitoring of the soil water inventory in agricultural fields is of high importance towards more efficient use of water in agricultural fields. In this thesis we tackled two related challenges: i) the development of a new method to objectively define the optimal number and tentative location of soil moisture sensors in agricultural fields based on soil moisture-based management zones, and ii) the use of a parsimonious semi-empirical exponential filter model to estimate rootzone soil moisture solely from a single soil moisture sensor located near the soil surface.

In the first study, we investigated the use of in situ soil moisture observations to delineate field management zones and guide the optimal deployment of soil moisture sensors in agricultural fields under rainfed and irrigated conditions. The proposed method revealed management zones (MZ) with distinct soil moisture regimes in all three fields, where direct soil moisture observations effectively captured the wetter and drier areas of the field. Management zones were delineated using an unsupervised clustering approach that reduced the intra-zone soil moisture spatial variability by about 50% compared to that in the entire field. Then we devised a quantitative method to objectively define the tentative location of soil moisture sensors avoiding field edges and transitioning areas between zones. Our work provides an objective methodology to guide the deployment of a limited number of soil moisture sensors across agricultural field. The study presented three main limitations, the first one related to the concentrations of soil moisture information on the top 12 cm of the soil profile without considering soil moisture at deeper layers which potentially could affect the delineation of the field MZ. The second limitation is the concentration of soil moisture surveys in intermediate to high field-average soil moisture conditions and the lack of surveys in drier (<0.247 m^3 m^{-3}). Finally, the third limitation is that our dataset of soil moisture observations was limited to periods with no vegetation. Previous studies have shown that the impact of plant water uptake on the soil moisture spatial variability is non-negligible. Future studies aiming at optimizing the number and deployment location of soil moisture sensors should explore soil moisture interactions with deeper soil layers across root-zone to provide a better understanding of the sub-surface spatial variability as well as incorporate rootzone soil moisture dynamics during the growing season.

The second study provided useful insights to estimate rootzone soil moisture from near surface soil moisture observations using a semi-empirical exponential filter model. Estimated rootzone soil moisture had an average RMSE of 0.049 $m^3\ m^{-3}$ across four sites. The exponential filter model resulted suitable for estimating rootzone soil moisture in only two out of four locations and performed particularly well in fields with a single crop during the study period. Based on our findings, the exponential filter model does not seem adequately predict rootzone soil moisture conditions in fields under crop rotations including multiple crops and fallow periods using single optimized *T* parameter. Two important limitations of this study are related to the lack of information of soil texture and root length at different profile depths. Differences is soil texture and soil physical properties across the soil column directly affect the performance of the exponential filter, thus soil texture data is a key to understand model results. Future work may be needed to fine-tune the exponential filter model to capture the contrasting and complex soil moisture conditions that can occur in agricultural fields by optimization the time length parameter for each phase of the crop rotation in order to improve the model predictions during the crop seasons.

Appendix A - Sensor Location Sensitivity

Table A.1. Pearson correlation between proxy variables used to evaluate sensor location sensitivity on each field. Wettest and driest observed soil moisture surveys, field elevation, and measured clay, sand, and silt content.

Field		Wettest	Driest	Elevation	Clay	Sand	Silt
A	Wettest	1	0.79	-0.32	0.74	-0.53	0.09
	Driest		1	-0.32	0.63	-0.34	-0.07
	Elevation			1	-0.31	0.06	0.18
	Clay				1	-0.69	0.09
	Sand					1	-0.78
	Silt						1
B	Wettest	1	0.51	-0.35	0.34	-0.51	0.51
	Driest		1	-0.29	0.21	-0.43	0.48
	Elevation			1	-0.42	0.38	-0.3
	Clay				1	-0.78	0.53
	Sand					1	-0.94
	Silt						1
C	Wettest	1	0.67	0.51	0.67	-0.63	0.31
	Driest		1	0.35	0.64	-0.43	0.1
	Elevation			1	0.25	-0.73	0.68
	Clay				1	-0.49	-0.05
	Sand					1	-0.85
	Silt						1

Table A.2. Sensor location coordinates base on different input variables for each management zone (MZ) in Field A. Distance values represent the discrepancy of sensor locations compared to the ground truth using all the soil moisture surveys (All SM).

Input Variables†	MZ	Latitude	Longitude	Distance	Total distance
				m	m
All SM	Dry	38.717	-97.435	0	0
All SM	Wet	38.716	-97.436	0	
Driest SM + Wettest SM	Dry	38.717	-97.434	12	91
Driest SM + Wettest SM	Wet	38.717	-97.436	79	
SM + Elev	Dry	38.717	-97.434	12	91
SM + Elev	Wet	38.717	-97.436	79	
SM + Elev + Clay + Sand	Dry	38.715	-97.434	199	662
SM + Elev + Clay + Sand	Wet	38.712	-97.435	463	
SM + Clay + Sand	Dry	38.715	-97.434	199	662
SM + Clay + Sand	Wet	38.712	-97.435	463	
Elev	Dry	38.716	-97.435	146	593
Elev	Wet	38.712	-97.435	447	
Elev + Clay + Sand	Dry	38.715	-97.434	199	662
Elev + Clay + Sand	Wet	38.712	-97.435	463	
Clay + Sand	Dry	38.715	-97.434	199	662
Clay + Sand	Wet	38.712	-97.435	463	

† SM = soil moisture survey and Elev = elevation above sea level.

Table A.3. Sensor location coordinates base on different input variables for each management zone (MZ) in Field B. Distance values represent the discrepancy of sensor locations compared to the ground truth using all the soil moisture surveys (All SM).

Input Variables†	MZ	Latitude	Longitude	Distance	Total distance
				m	m
All SM	Dry	37.967	-97.882	0	0
All SM	Wet	37.965	-97.879	0	
Driest SM + Wettest SM	Dry	37.967	-97.883	76	90
Driest SM + Wettest SM	Wet	37.965	-97.879	14	
Driest SM + Wettest SM	Dry	37.967	-97.883	76	90
SM + Elev	Wet	37.965	-97.879	14	
SM + Elev	Dry	37.967	-97.882	68	204
SM + Elev + Clay + Sand	Wet	37.965	-97.878	136	
SM + Elev + Clay + Sand	Dry	37.967	-97.882	68	204
SM + Clay + Sand	Wet	37.965	-97.878	136	
SM + Clay + Sand	Dry	37.966	-97.883	185	293
Elev	Wet	37.966	-97.879	108	
Elev	Dry	37.966	-97.882	95	209
Elev + Clay + Sand	Wet	37.965	-97.878	114	
Elev + Clay + Sand	Dry	37.966	-97.882	95	209
Clay + Sand	Wet	37.965	-97.878	114	

† SM = soil moisture survey and Elev = elevation above sea level.

Table A.4. Sensor location coordinates base on different input variables for each management zone (MZ) in Field C. Distance values represent the discrepancy of sensor locations compared to the ground truth using all the soil moisture surveys (All SM).

Input Variables†	MZ	Latitude	Longitude	Distance	Total distance
				m	m
All SM	Dry	38.205	-97.568	0	0
All SM	Wet	38.209	-97.568	0	
Driest SM + Wettest SM	Dry	38.205	-97.567	17	164
Driest SM + Wettest SM	Wet	38.209	-97.568	147	
Driest SM + Wettest SM	Dry	38.205	-97.568	17	164
SM + Elev	Wet	38.208	-97.567	147	
SM + Elev	Dry	38.205	-97.567	48	85
SM + Elev + Clay + Sand	Wet	38.209	-97.568	37	
SM + Elev + Clay + Sand	Dry	38.205	-97.567	48	85
SM + Clay + Sand	Wet	38.209	-97.568	37	
SM + Clay + Sand	Dry	38.205	-97.567	54	91
Elev	Wet	38.209	-97.568	37	
Elev	Dry	38.205	-97.567	48	85
Elev + Clay + Sand	Wet	38.209	-97.568	37	
Elev + Clay + Sand	Dry	38.205	-97.567	48	85
Clay + Sand	Wet	38.209	-97.568	37	

† SM = soil moisture survey and Elev = elevation above sea level.

Appendix B - Soil Moisture probability distribution

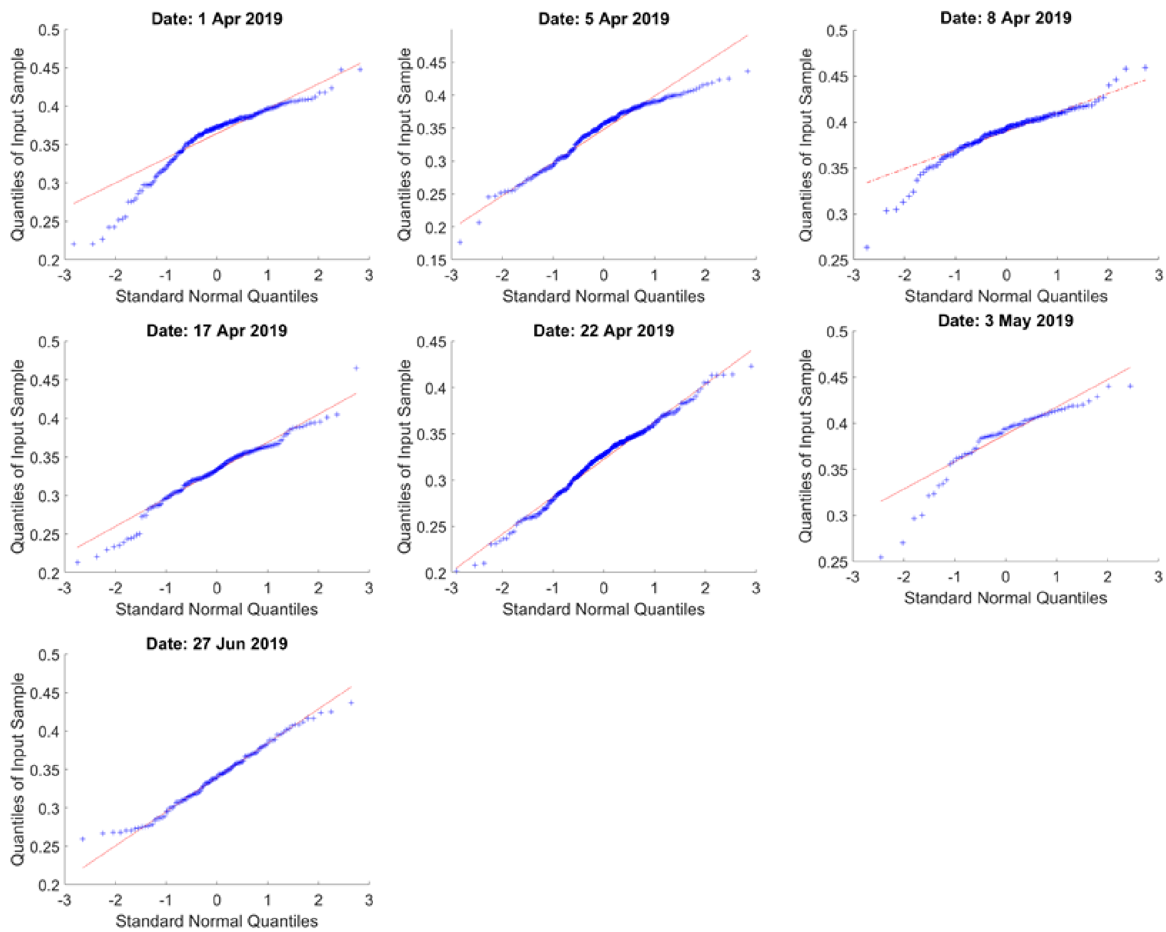

Figure B.1. Quantile-Quantile plots showing the probability distribution of intensive soil moisture surveys for Field C.